AD-A072 600 BATTELLE COLUMBUS LABS DURHAM N C F/G 17/1
ON THE DETERMINATION OF ARRIVAL TIMES FOR SOUND RANGING. I. EFF--ETC(U)
MAY 79 E A DEAN DAAG29-76-D-0100

UNCLASSIFIED ERADCOM/ASL-CR-79-0100-2 NL

1 OF 1
AD
A072600

END
DATE FILMED
9-79
DDC

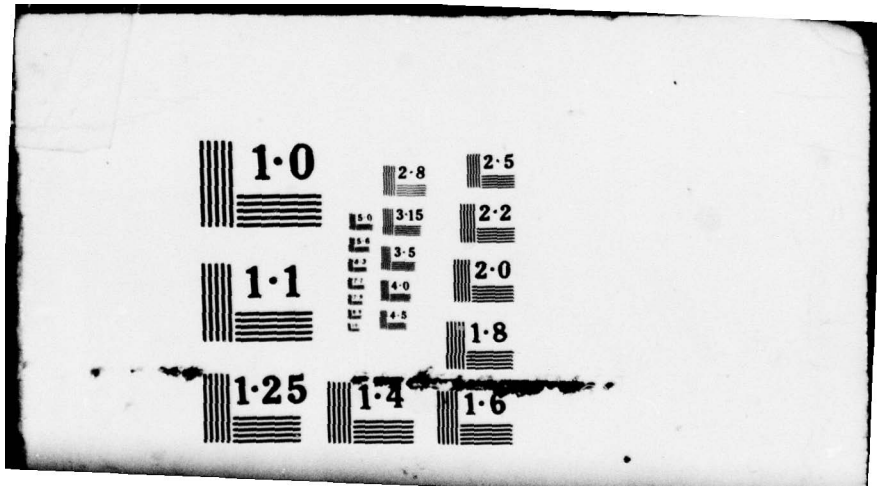
1·0
1·1
1·25
1·4
1·6
1·8
2·0
2·2
2·5
2·8
3·15
3·5
4·0
4·5
5·0

ASL-CR-79-0100-2

ON THE DETERMINATION OF ARRIVAL TIMES FOR SOUND RANGING I. EFFECTS OF FINITE AMPLITUDE PROPAGATION, VERTICAL METEOROLOGICAL GRADIENTS, AND SYSTEM TRANSIENT RESPONSE

May 1979

Prepared by

E.A. DEAN
Physics Department
The University of Texas at El Paso
El Paso, Texas 79968

Under Contract No. DAAG29-76-D-0100
Contract Monitor: ABEL J. BLANCO

Approved for public release; distribution unlimited

US Army Electronics Research and Development Command
ATMOSPHERIC SCIENCES LABORATORY
White Sands Missile Range, NM 88002

NOTICES

Disclaimers

The findings in this report are not to be construed as an official Department of the Army position, unless so designated by other authorized documents.

The citation of trade names and names of manufacturers in this report is not to be construed as official Government indorsement or approval of commercial products or services referenced herein.

Disposition

Destory this report when it is no longer needed. Do not return it to the originator.

SECURITY CLASSIFICATION OF THIS PAGE *(When Data Entered)*

REPORT DOCUMENTATION PAGE

READ INSTRUCTIONS BEFORE COMPLETING FORM

1. REPORT NUMBER: ASL-CR-79-0100-2	2. GOVT ACCESSION NO.
3. RECIPIENT'S CATALOG NUMBER: ERADCOM/ASL	
4. TITLE (and Subtitle): ON THE DETERMINATION OF ARRIVAL TIMES FOR SOUND RANGING. I. EFFECTS OF FINITE AMPLITUDE PROPAGATION, VERTICAL METEOROLOGICAL GRADIENTS, AND SYSTEM TRANSIENT RESPONSE	5. TYPE OF REPORT & PERIOD COVERED
	6. PERFORMING ORG. REPORT NUMBER
7. AUTHOR(s): E. A. Dean	8. CONTRACT OR GRANT NUMBER(s): DAAG29-76-D-0100
9. PERFORMING ORGANIZATION NAME AND ADDRESS: Physics Department, The University of Texas at El Paso, El Paso, Texas 79968	10. PROGRAM ELEMENT, PROJECT, TASK AREA & WORK UNIT NUMBERS: DA Task No. 1L162111AH71/26
11. CONTROLLING OFFICE NAME AND ADDRESS: US Army Electronics Research and Development Command, Adelphi, MD 20783	12. REPORT DATE: May 1979 13. NUMBER OF PAGES: 61
14. MONITORING AGENCY NAME & ADDRESS *(if different from Controlling Office)*: Atmospheric Sciences Laboratory, White Sands Missile Range, NM 88002	15. SECURITY CLASS. *(of this report)*: UNCLASSIFIED 15a. DECLASSIFICATION/DOWNGRADING SCHEDULE

16. DISTRIBUTION STATEMENT *(of this Report)*

Approved for public release; distribution unlimited

17. DISTRIBUTION STATEMENT *(of the abstract entered in Block 20, if different from Report)*

18. SUPPLEMENTARY NOTES

Contract Monitor: Abel J. Blanco

19. KEY WORDS *(Continue on reverse side if necessary and identify by block number)*

Sound ranging
Atmospheric propagation
Meteorological corrections
Shock wave
Microphone

20. ABSTRACT *(Continue on reverse side if necessary and identify by block number)*

Several factors bearing on the determination of arrival times in sound ranging are investigated. These factors include the propagation of a finite amplitude triangular shock wave, the diffraction due to the surface and the refraction due to the phase velocity increasing with height, and the effect of the microphone response. Corrections are derived for finite amplitude effects and refraction under a constant gradient for sound speed and wind speed. Recommendations for experimental studies to confirm this theoretical work are included.

DD FORM 1 JAN 73 1473 EDITION OF 1 NOV 65 IS OBSOLETE

391 859

SECURITY CLASSIFICATION OF THIS PAGE *(When Data Entered)*

79 08 10 019

TABLE OF CONTENTS

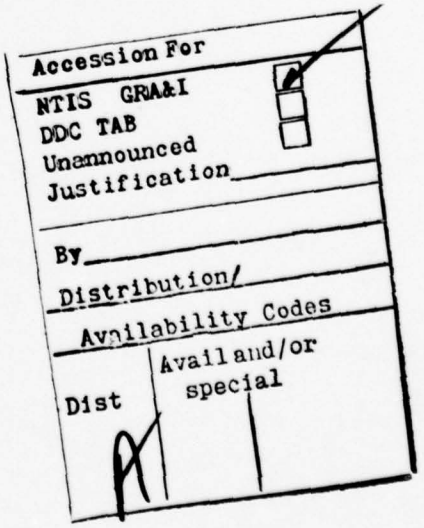

INTRODUCTION

Assume an explosive source located at $\vec{R}$, with coordinates X and Y, occurring at time T. The resulting wave may be described by rays which are normal to the wave front and which travel with velocity $c\hat{n} + \vec{w}$, where c is the mean sound speed, $\hat{n}$ is the unit vector in the direction of propagation relative to the air, and $\vec{w}$ is the wind velocity, with x- and y-components u and v. The wave arrives at a microphone M_i located at $\vec{r}_i = (x_i, y_i)$ at time t_i. The following vector equality holds:

$$\vec{R} + (c_i\hat{n}_i + \vec{w}_i)\ (t_i - T) = \vec{r}_i, \tag{1}$$

where c_i and $\vec{w}_i$ are mean speeds over the path from the source to M_i. When Eq. (1) is solved for $c\hat{n}_i(t_i-T)$, and resolved into component form,

$$c_i^2(t_i - T)^2 = [X-x_i + u_i(t_i - T)]^2 + [Y - y_i + v_i(t_i - T)]^2. \tag{2}$$

Formally, one has

$$f_i(X,Y,T) = 0,\ i = 1,2,\ldots n, \tag{3}$$

if there are n microphones.

The system of non-linear equations represented by Equation (3) requires three microphones for a solution of X, Yand T. More than three microphones form an over-determined system. To completely locate the source requires accurate knowledge of c_i, $\vec{w}_i$, $\vec{r}_i$, and t_i.

Devoting attention to the problem of determining t_i alone, without the consideration of the complete problem could be merely an academic exercise.

First, it is obvious that the error in determining the source position is dependent on all the quantities c_i, $\vec{w}_i$, $\vec{r}_i$, and t_i. A surveying error of one foot toward the source is equivalent to one msec time error. The quantities c_i and $\vec{w}_i$ must be considered means over the individual ray paths, which do not necessarily follow the surface. Second, the problem of what is the "best" solution to an over-determined system of equations is not clear. The present method appears to weight the end microphones by one-half. Should a weighted least-squares method be used, or perhaps a "robust" method which is insensitive to large errors in individual microphones? An empirical test of the "best" determination of t_i is not independent of the algorithm used in solving Equation (3). Third, the nature of the signal is changed by the propagation through the air and by the detection and recording system. This fact severely affects the determination of t_i.

Thus certain areas of the entire sound ranging problem -- those areas which appear to directly affect the determination of arrival times -- will be investigated. The total problem is shown as a block diagram in Figure 1. The source is characterized by its position X and Y, time T and energy E. This produces some disturbance in time f(t). This disturbance is propagated through the atmosphere, which acts as a non-linear filter, producing a different signal h(t). This filter may be characterized by its sound speed c, a function of time, position, and height and by the ratio of the specific acoustic impedance of the surface to that of air, Z. The microphone detects this signal and whatever noise is available. The microphone, the amplifier, and the recorder also act as a filter, with response $g(\omega)$, changing the signal to q(t). It is this signal which provides the information from which the arrival time at each microphone must be determined. The arrival times, together with surveying and

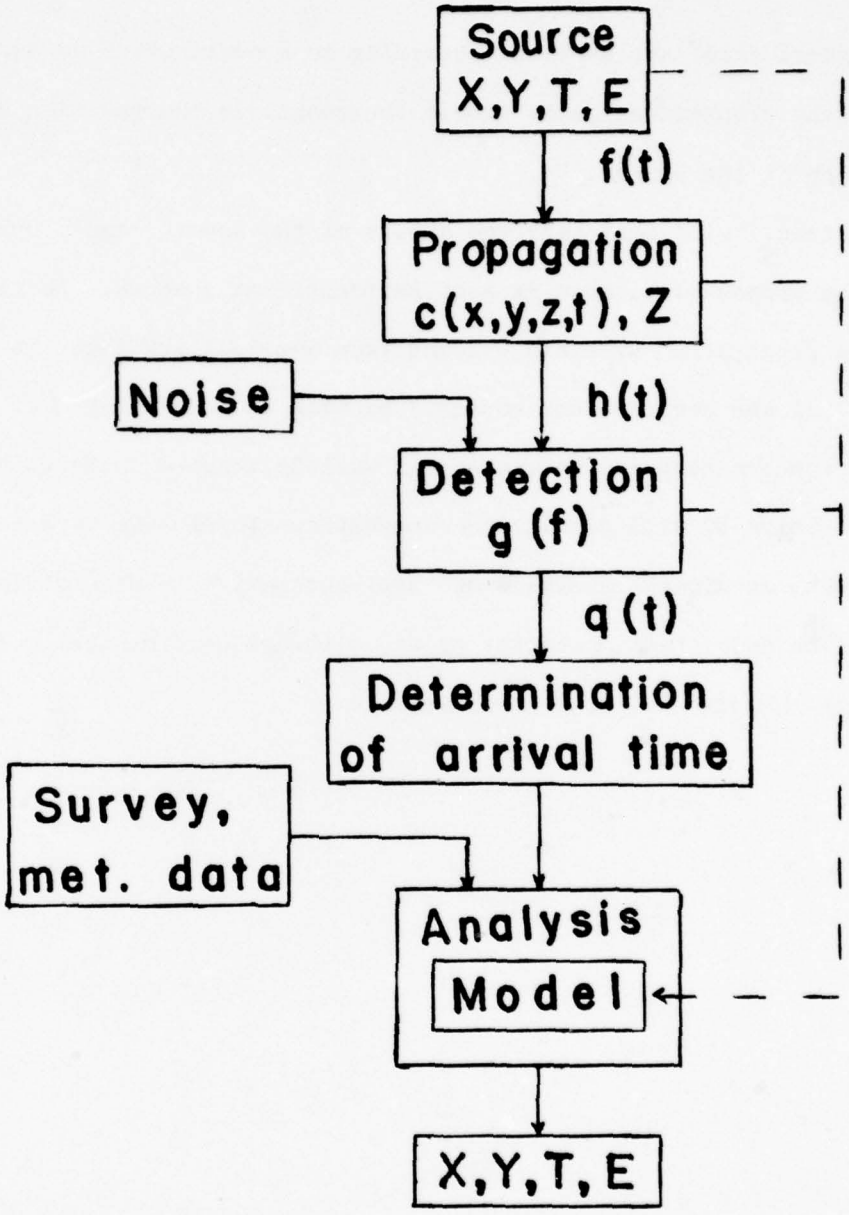

Figure 1. Block diagram of sound ranging problem. The dashed lines indicate the theoretical connections by means of a model. At present, there are no connections from source or detection.

meteorological data, are analyzed according to a model which is supposed to represent the propagation delay time. The result is the position and perhaps the strength of the source.

Section I will deal with the nature of the source signal during the early part of the propagation, when it must be treated as a shock. Section II considers the propagation problems arising from vertical gradients in temperature and wind, and the ever-present boundary between the earth and air. The effect of the microphone response on the signal will be treated in Section III. Finally, Section IV will contain recommendations for future investigations. Some attempts at digital analysis and semi-automation in determining arrival times will be described in another paper, although some general comments on this subject are included in the recommendations.

I. THE PROPAGATION OF AN EXPLOSIVE SHOCK WAVE

The propagation of explosive shocks in the atmosphere has received extensive investigation during the last 30 years.[1] Both theoretical calculations and experimental measurements over wide ranges of explosive energies agree that, after a certain distance, the disturbance is described by the pressure vs length signal shown in Figure 2. Both the magnitude of the pressure rise P and the length of the positive pressure pulse L are functions of the dimensionless variable $\zeta = r/d$, where r is the distance from the source and d is a characteristic length given by

$$d = (E/P_o)^{1/3}, \tag{4}$$

where E is the energy of the source and p_o is the ambient atmospheric pressure.

Less is known about the negative pressure region. The magnitude and length described in Figure 2 are taken from Brode[2]. Sometimes secondary reflected pulses ride along this region. However, the initial pressure surge and the length of this pulse are certainly the important parameters of the signal in determining arrival time. Surely if this signal were not distorted by the atmosphere, ground, and microphone, the determination of arrival times would be simplified.

The characteristic length given by Equation (4) is proportional to the cube root of the energy of the charge propelling the projectile less the energy of the projectile and recoil, thus approximately proportional to the diameter of the bore. However, for artillery, various lengths of charge are available. Using values reported by Wurtele and Roe[3], the energy for the No. 7 charge for an 8-in bore is 1.22×10^8 J. For sea-level, this results in d = 10.6 m. Other charges and bores of US artillery have energies which may be approximately by

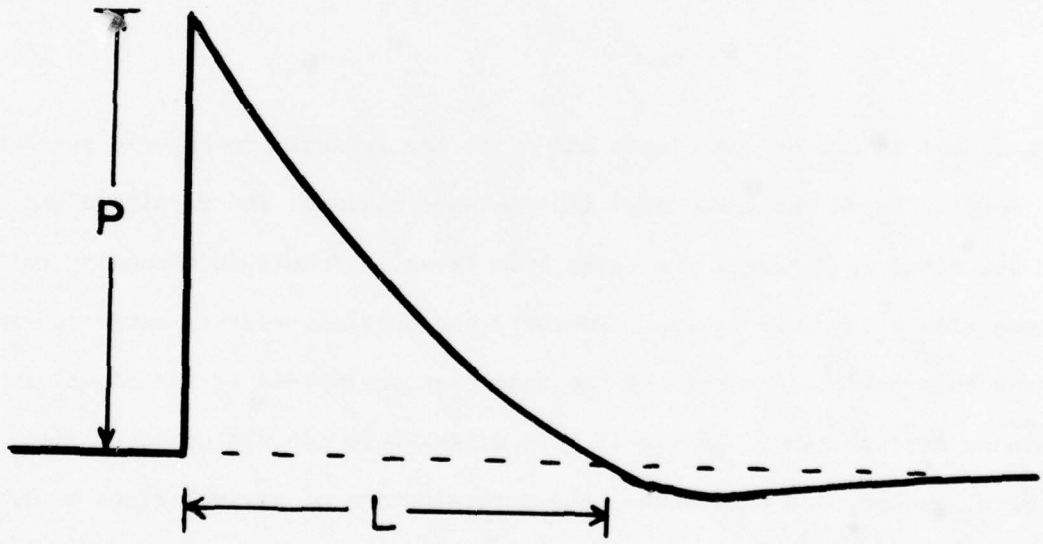

Figure 2. Overpressure vs. length for a typical wave due to an explosive source. P is the shock pressure differential and L is the length of the overpressure pulse.

scaling to the kinetic energy of the projectile, given by the weight and muzzle velocity. Table 1 contains the resulting characteristic lengths for charges N No. 1 through No. 7 for 8-in, 155-mm and 105-mm artillery. It may be noted that there is overlap, depending on the charge used, between light and medium and between medium and heavy artillery.

Table 1. Characteristic lengths for various charges and diameters. (Length in meters.)

Diam.	Charge #1	Charge #3	Charge #5	Charge #7
105 mm	2.9	3.3	3.9	5.2
155 mm	4.1	4.9	6.0	8.0
8 in	5.9	6.8	8.4	10.6

At the range of 1 km, Table 1 yields a dimensionless parameter ζ which varies between 94 for the most powerful 8-in charge and 350 for the least powerful 105-mm charge. The largest value expected would be for No. 7, 105-mm at maximum range (11.5 km), which is $\zeta \approx 2200$. Thus the range of ζ of interest in sound ranging is from 100 to 2000. For these values of ζ, the shock is weak and the compilation by Baker is incomplete; his values for L beyond $\zeta = 60$ being an extrapolation. Fortunately the shock is weak, allowing the calculation of wave-shapes and arrival times.

The detail of this calculation are relegated to Appendix A. Due to the quasi-adiabatic nature of the propagation, the high-pressure shock front travels faster than the ambient pressure point on the wave. The rate at which L increases with distance of propagation is given approximately by

$$\frac{dL}{dr} = \frac{\gamma+1}{4\gamma} \frac{P}{p_o} \qquad (5)$$

where γ is the ratio of specific heats (1.40 for air) and P is the peak overpressure. The increase in entropy across the weak shock causes the total energy of the wave to decrease with the distance of propagation according to

$$\frac{1}{E}\frac{dE}{dr} = -\frac{\gamma+1}{4\gamma}\frac{P}{p_o}\frac{1}{L}, \tag{6}$$

where E is the energy of the wave, given by

$$E = \frac{4\pi r^2 P^2 L}{3\rho c^2} \tag{7}$$

here ρ is the air density and c is the sound speed.

The substitution of Equation (5) into Equation (6) and the integration of the result yields

$$EL = \text{constant}. \tag{8}$$

Equation (7) and (8) may be solved for P as a function of r and L,

$$P = P_o\ (r_o/r)\ (L_o/L), \tag{9}$$

where the zero subscripts refer to some reference distance from the source, r_o. Finally, Equation (5) combined with Equation (9) may be integrated to obtain:

$$L = \sqrt{L_o}[L_o + \frac{\gamma+1}{4\gamma}\frac{P_o}{p_o}\ r_o\ \ln(r/r_o)]^{1/2}. \tag{10}$$

Using Baker's tabulated values for $\zeta = 60$, ($P_o/p_o = 2.48 \times 10^{-3}$, $L_o = 0.8561$, $r_o = 60d$), one has

$$L(\zeta) = d[0.733 + 0.109\ \ln\ (\zeta/60)]^{1/2}. \tag{11}$$

Several values of this function and others of interest in sound ranging are tabulated in Table 2. The relative overpressures P/p_o are determined from

Equation (9). The next column contains the instantaneous speed of the wave (V/c) as a function of ζ. This is calculated from

$$V = c\left(1 + \frac{\gamma+1}{4\gamma}\frac{P}{p_o}\right) , \qquad (12)$$

derived in Appendix A. One notes that this speed is very close to the speed of sound.

The important speed in the sound ranging equations is, however, not the instantaneous speed, but the mean speed over the path. Due to the strong shock propagation close to the source, the mean speed is larger than the instantaneous speed. The last column of Table 2 lists this mean speed as a function of ζ. For $\zeta = 60$, Baker gives for the arrival time $t = 58.8c$, or $\langle V\rangle/c = 1.020$. The mean speeds in Table 2 are based on this plus the change in arrival time due to ΔL between ζ values. The tabulated values are given quite accurately by the empirical fit

$$\langle V\rangle/c = 1 + 1.4/\zeta - 15/\zeta^2 \qquad (13)$$

over the range $\zeta = 100$ to $\zeta = 2000$. It may be noted that these values are not negligible for heavy artillery at short ranges, varying between a 1.25% correction to a 0.39% correction for heavy to light artillery at 1 km. This is equivalent to temperature corrections of 1.9°C and 0.2°C respectively.

Table 2. Dimensionless variables for the propagation of explosive shocks. The characteristic length is $d = (E/p_o)^{1/3}$. The characteristic speed is the sound speed c.

$\zeta = r/\ell$	L/d	P/p_o	v/c	$\langle v\rangle/c$
100	0.893	1.43×10^{-3}	1.00061	1.0125
200	0.941	6.77×10^{-4}	1.00029	1.0065
500	1.002	2.54	1.00011	1.0027
1000	1.045	1.22	1.00005	1.0014
2000	1.086	5.86×10^{-5}	1.00003	1.0007

In principle, a faithfully received signal, together with a known range, would allow the determination of d and hence the energy of the source. In practice, the vagaries of propagation close to the earth's surface make this determination exceedingly difficult. The most useful information is probably contained in the period or frequency content, rather than the pulse height. Assuming a mean value of L/d to be 1, the period of the positive pulse will be approximately d/c. The characteristic lengths in Table 1 show that heavy artillery will have periods ranging from 17 to 31 msec, medium artillery will range from 12 to 24 msec, and light artillery will range from 9 to 15 msec in period in the order of 12 msec.

The frequency spectrum of a signal such as shown in Figure 2 is obtained from the Fourier transform of the pulse,

$$p(\omega) = \int_{-\infty}^{\infty} P(t)\, e^{i\omega t} \tag{14}$$

where ω is the angular frequency $2\pi f$. For a pulse approximating Figure 2,

$$P(t) = \begin{cases} 0 & , \quad t<0 \\ P_o(1-t/\tau), & 0<t<\tau \\ 0 & , \quad t>\tau \end{cases} , \tag{15}$$

$$\left|\frac{P(\omega)}{P_o \tau}\right| = \frac{1}{\omega\tau}\left[\left(1 - \frac{\sin\omega\tau}{\omega\tau}\right)^2 + \left(\frac{1-\cos\omega\tau}{\omega\tau}\right)^2\right]^{1/2} \tag{16}$$

This relative spectrum is shown in Figure 3. The high frequency spectrum falls off at 6 db per octave, being down 3 db at $\omega\tau \simeq 5$. This 3-db point corresponds to a frequency of $0.8/\tau$, where τ is the over-pressure period. This frequency ranges from 26 to 46 Hz for heavy, 34 to 66 Hz for medium, and 52 to 94 Hz for light artillery.

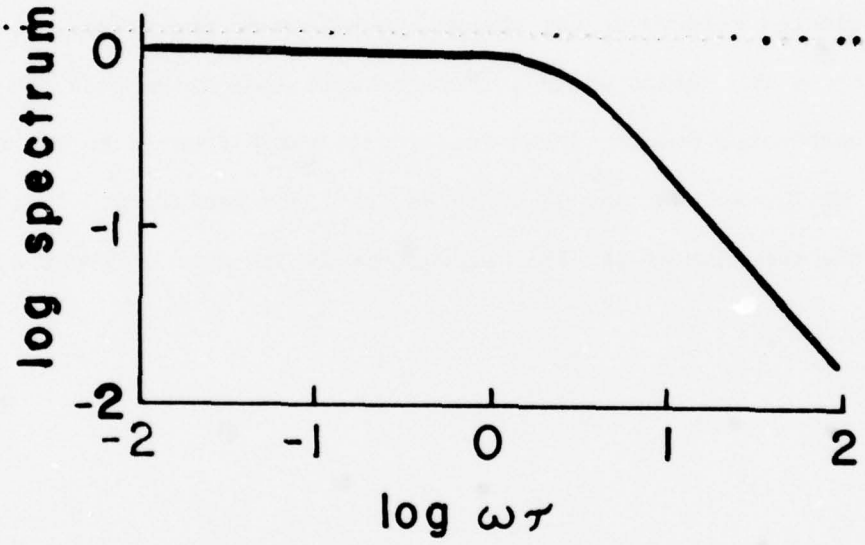

Figure 3. The magnitude of the pressure spectrum of a pulse such as shown in Figure 2. The period of the pulse is T = L/c. The high frequency rolls off at 6 db/octave with the -3 db point at about ωT = 5.

The above theoretical predictions for the wave shapes due to various artillery assume spherical propagation through a homogeneous, non-absorbing medium with no boundaries. Perhaps the two most dangerous assumptions involve the neglect of absorption and the neglect of boundary influence. Both of these neglected effects tend to filter out the high frequencies of the wave, although the fundamental over-pressure period ought not be effected much. These effects then primarily increase the rise time of the initial pressure pulse, although the finite amplitude effect considered here will tend to reshape the shock.

Since the neglected effects do not change the period of the pulse, the fundamental frequency of the period would perhaps be more indicative than the 3-db points of the unabsorbed pulse. These frequencies range from 16 to 20 Hz for heavy, 21 to 41 Hz for medium, and 33 to 59 Hz for light artillery. Section III will show that the response of the T-23 microphone is 3db down at about 25 Hz.

II. ATMOSPHERIC PROPAGATION OF THE PULSE

The sound ranging equation, Eq. (2) is a two-dimensional equation, assuming circular propagation in a plane. This plane is, of course, the surface of the earth where both the source and receivers are located. Disregarding that this surface is not often a plane to within the wavelengths involved, and assuming a homogeneous surface temperature and wind, there still exists the problem of temperature and wind variations with altitude. It is well known that these variations cause waves to be refracted -- sometimes upward resulting in the microphone being in a shadow zone, sometimes downward resulting in direct propagation along a curved path. (See Figure 4.) Thus two cases exist: If the phase velocity of sound decreases with altitude, only diffracted energy reaches the microphone, traveling with the speed determined by the surface temperature and wind. As is true for all diffracted waves, the low frequency components are diffracted with greater efficiency than the high frequency components. The second case of refracted propagation occurs if the phase velocity increases with altitude. Due to Fermat's principle, the curved path results in a travel time which is less than the path along the surface. This results in a higher mean velocity than that predicted by use of the surface temperature and wind. In addition, reflections from the ground make possible multiple paths, with the corresponding superposition of signals.

The diffracted case is mathematically difficult and is also beset with experimental difficulties involving the determination of the specific acoustic impedance of the surface, not to mention the large number of different geological and biological surfaces imaginable. Wurtele and Roe[3], using Doak's solution[4], have determined the effect of the boundary on the shape of pulses described by Heaviside step functions and "N" shaped waves. Their results indicate the

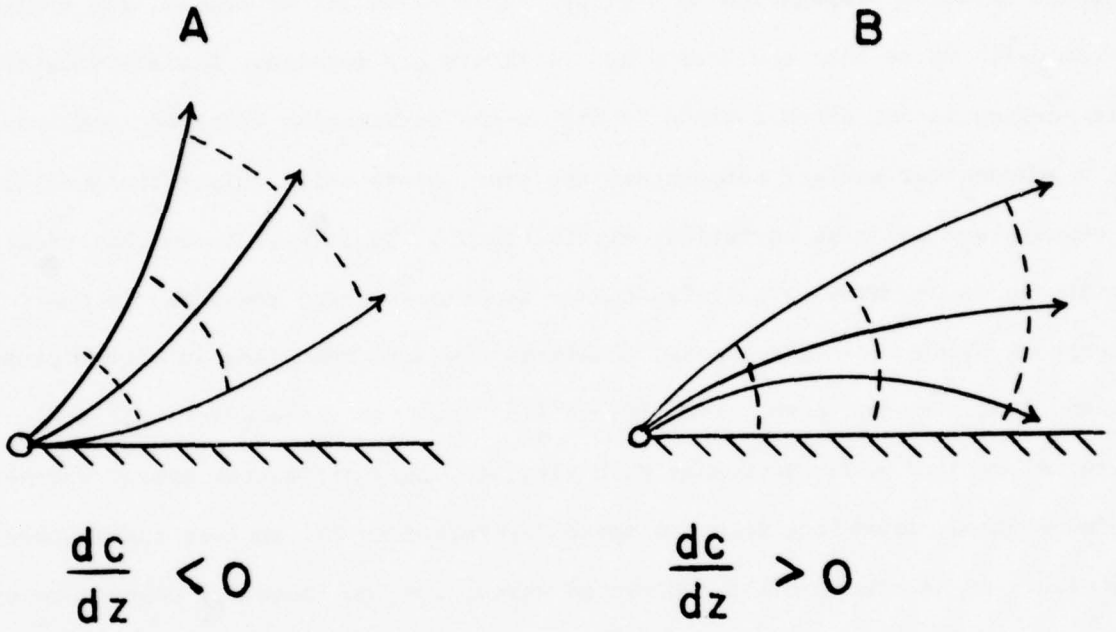

Figure 4. Propagation for (A) gradient in phase velocity is negative, and (B) gradient in phase velocity is positive. Case A creates a shadow zone along the surface however sound is diffracted (with loss of high frequency components) along the surface. Case B results in the refracted ray arriving before a surface ray would arrive.

rather drastic filtering effects on pulses diffracted over boundaries which have specific acoustic impedances that are not much larger than that of air. Figure 5 (adapted from their Figure 4.5) shows the resulting shape of an "N" shaped wave of 29 msec duration after being diffracted one km along surfaces of various specific acoustic impedances. In the figure, Z is the ratio of the surface impedance to that of air, ρc.

Although the signal is fairly faithfully reproduced for Z = 100, lesser values of Z show increasingly severe loss of high frequency components. The boundary thus acts as a low-pass filter, reducing the amplitude of the signal and increasing the uncertainty in determining the arrival time, although the original pulse length is preserved. The rise time increases with distance, as shown in Fig. 6, where a unit step function is shown after being propagated according to Wurtele and Roe for distances of 1, 2, 5, and 10 km along a surface with Z = 10. Consideration of the fact that artillery pulses are not longer than 30 msec leads to the conclusion that arrival times are increasingly difficult to measure for longer distances.

Even though diffracted signals may (dependent upon Z and range) make source strength determination and arrival time difficult to measure, the propagation along the surface simplifies the determination of mean sound speed. The proper values to use when the phase velocity decreases with height are simply the surface values of temperature and wind velocity. There appears to be no need to include upper-level values in some weighting scheme.

In cases where the phase velocity increases with height, the situation is reversed. The refracted waves ought to faithfully represent the pulse investigated in Section I, but the mean sound speed and wind velocity must include the properly weighted upper-level meteorological data. These mean values could

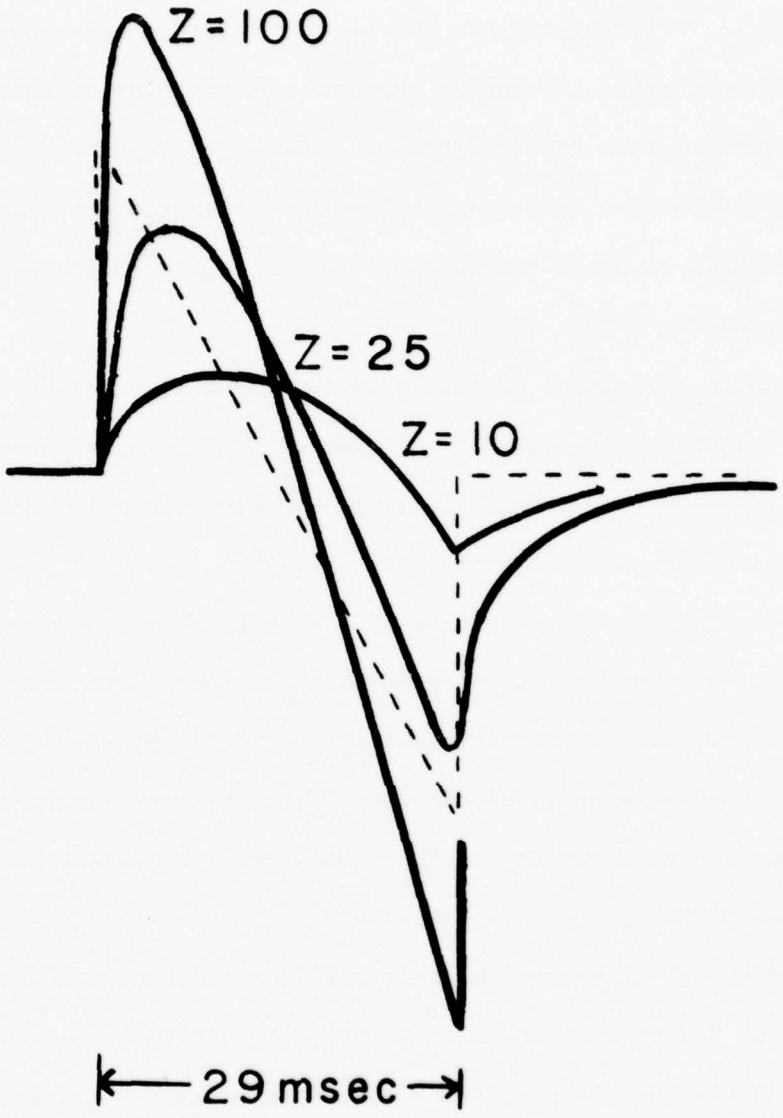

Figure 5. Distortion of 29 msec "N" shaped pulse after being propagated 1 km. (Adapted from Wurtele & Roe, 1977.) The ratio of the specific acoustic impedances of the surface to that of the medium is Z.

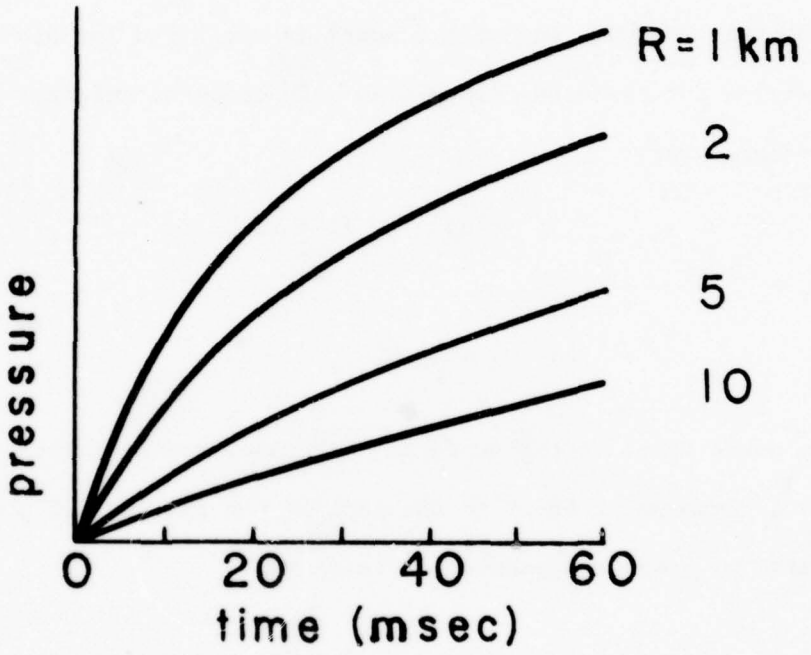

Figure 6. Rise times for a Heaviside step function diffracted along boundary of Z = 10 for various distances. (Adapted from Wurtele and Roe, 1977).

be determined by a ray-tracing program, but that would probably require too much computer power. An approximation to the correct weighting may be obtained for simple atmospheric models. The simplest model is one in which it is assumed that both the sound speed and wind vectors have linear gradients with respect to height.

The analytic solution for such a model is contained in Appendix B. If a Taylor expansion for the sound speed c as a function of height z is truncated at the first-degree term,

$$c(z) = c_o\ (1 + az), \tag{17}$$

where

$$a = \frac{1}{c_o}\frac{dc}{dz}\ , \tag{18}$$

and c_o is the sound speed at the surface. Likewise, the wind vector, when resolved into a component tangent to the path of the ray (u) and a component normal to the path (v), may be expanded to yield:

$$\begin{aligned} u(z) &= u_o + c_o bz, \\ v(z) &= v_o + c_o dz, \end{aligned} \tag{19}$$

where

$$b = \frac{1}{c_o}\frac{du}{dz}\ , \quad d = \frac{1}{c_o}\frac{dv}{dz}\ .$$

Under the assumption that higher-order terms are negligible, it is shown in Appendix B that the mean speeds for a refracted ray are given by the values c, u, and v evaluated at one-third of the maximum height of the ray, and that the maximum height obtained by the ray is given by

$$Z = \frac{1}{8}\ (a + b)\ R^2, \tag{20}$$

where a and b are the gradients defined above, and R is the range of the ray (the distance between source and receiver). It is clear from Equation (20) that Z is positive only if $a + b > 0$. Otherwise the ray is diffracted along the boundary rather than refracted along a curved path.

Table 3. Meteorological variables for first example.

Parameter	Surface	800 m-level
Virtual temp.	280 K	275 K
East wind	0	5 m/sec
North wind	0	2 m/sec

As an example, suppose the virtual temperature and wind components are given by Table 3. One has $C_o = 20.05\ (280)^{1/2} = 335.5$ m/sec, $c_{800} = 332.5$ m/sec, $a = -1.12 \times 10^{-5}\ m^{-1}$, $b = -1.86 \times 10^{-5}\ m^{-1}$ (along the x-axis), and $d = +0.75 \times 10^{-5}\ m^{-1}$. Propagation in most directions is along the surface, with c = 335.5 m/sec. However, propagation in the negative x-axis (toward the west, down wind from the east wind) is refracted. Here $a + b = 0.74 \times 10^{-5}\ m^{-1}$, yielding a maximum height of only one meter for a range of a km, and 92 m for a range of 10 km. Neither of these ranges would yield much of a change in mean sound speed, there being only a 0.1 m/sec change from the surface value in the latter case.

Table 4. Meteorological variables for second example. (Actual case at WSMR.)

Parameter	Surface	200 m-level
Virtual temp.	281.5 K	283.1 K
East wind	0	7 m/sec
South wind	0	2 m/sec

However, larger gradients are possible. Consider the case described by Table 4. One has for propagation in the westerly direction:

$$c_o = 336.4 \text{ m/sec}$$

$$c_{200} = 337.4 \text{ m/sec}$$

$$a = 1.49 \times 10^{-5} \text{ m}^{-1}$$

$$b = 10.4 \times 10^{-5} \text{ m}^{-1}$$

$$d = 3.0 \times 10^{-5} \text{ m}^{-1}$$

The mean speed along the direction of propagation is

$$\langle v_x \rangle = 336.4[1 + 5.9 \times 10^{-4} R^2],$$

where R is the range in km. For 1 km, $\langle v_x \rangle$ = 336.6 m/sec, and for 10 km, $\langle v_x \rangle$ = 356.2 m/sec, a 20 m/sec difference from v_o. For R = 1 km, Z = 15 m, and for R = 10 km, Z = 1.5 km (higher than the 200 m level, requiring knowledge of the meteorological parameters above 200 m). Since most temperature inversions do not prevail for 1.5 km, the R = 10 km case would not be as drastic as calculated above.

This method of approximation to the correct weighting of upper layer meteorological data is not significantly more difficult than the presently used method. For a particular ray, if $a + b < 0$, then surface values would be used. If $a + b > 0$, an analysis using surface values could be used to determine R, and Eq. (20) would yield the maximum height obtained. The meteorological data evaluated at one-third this height would then be used for hte mean sound speed determination.

Refracted propagation also opens the possibility of multiple arrivals. Some rays leaving the source at smaller elevation angles are refracted back to the surface where they are reflected and finally arrive at the receiver. These

rays arrive later than the main refracted ray, and with amplitudes dependent on the reflection coefficient at the surface and the angle of incidence. Since the maximum height depends on the square of the distance, the correction in the time of arrival depends on the inverse square of n + 1, where n is the number of reflections. Thus the travel time, which for the main refraction, is given by Eq. (B20).

$$T = \frac{R}{c_o} \left[1 + \frac{1}{24} (a + b)(a + 6b) R^2\right], \tag{21}$$

becomes

$$T = \frac{R}{c_o} \left[1 + \frac{1}{24} (a + b)(a + 6b) \left(\frac{R}{n+1}\right)^2\right] \tag{22}$$

for a refraction which is reflected n times. As n becomes large, T approaches R/C_o. These multiple arrivals should come in at times which are reminiscent of the hydrogen spectrum, since Equation (22) is of the same form as Rydberg's equation $(1/n^2)$.

Finally, Appendix B determines the mean sound speeds to be used in the sound ranging equations. These are not the same as the instantaneous speeds measured at the microphone array. Since the arriving ray comes in at an angle θ_o, the trace velocity of the wave as it crosses the array is faster than the mean speed between source and receiver. Snell's law requires that these trace velocities are in fact equal to the speed at the maximum height obtained by the ray. This may be determined by calculating

$$\frac{dx}{dt} = \frac{dx}{d\theta_o} \frac{d\theta_o}{dt} \quad , \tag{23}$$

which, using the results in Appendix B, results in

$$\left.\frac{dx}{dt}\right|_R = C_o\left[1 + (a + b)Z + \frac{u_o}{c_o}\right] \quad , \tag{24}$$

where Z is the maximum height obtained for the range R.

In the analysis of the sound ranging problem where the sound speed is a function of range, as it is both for the finite amplitude effect and the refracted effect, care must be exercised in the formation of the equations to assure that the travel times reflect the mean sound speed over the ray, rather than simple time differences determined by the local sound speed.

III. THE RESPONSE OF THE MICROPHONE

The T-23 microphone is basically a pair of Helmholtz resonators with heated wires inserted in the neck connecting the two resonators. As the air in this neck moves, wires change their temperature due to convection. These wires are part of a bridge circuit which develops an unbalanced electromotive force due to the change in resistance of the wires. Figure 7 indicates the physical layout of the resonators.

The equivalent electrical circuit for the double resonator is shown in Figure 8. The acoustical inertance of a neck is labled M, the acoustical resistance of a neck is labled R, and the acoustical stiffness of a cavity is labled C. It is apparent from Figure 8 that the bottom resonator acts as a series LC-tank circuit, with the top resonator acting as a low-pass filter.

From measured parameters of the microphones and from the actual response of several microphones as measured in a pistonphone, the frequency response of the microphone has been determined. The details of this determination are contained in Appendix C. The resulting response is illustrated in Figure 9. It is noted that the response is sharply peaked at about 17 Hz, with a -6db/octave roll-off for low frequencies and a -18db/octave roll-off for high frequencies. Comparing this response with the spectrum of the artillery pulse, as developed in Section I, confirms that the microphone's frequency response does not pass enough high frequency information to faithfully reproduce the signal.

The problem faced in increasing the frequency response of the microphone is that this will also increase the noise in the recorded signal. Whether the signal-to-noise ratio is improved by an extended frequency response depends on the nature of the noise spectrum. The noise spectrum, of course, depends on a lot of variables, including terrain, wind fluctuations, and man-made noise.

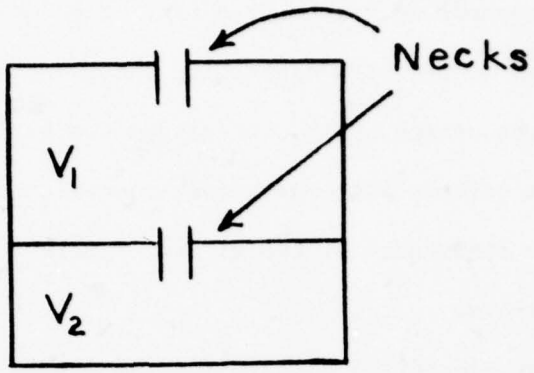

Figure 7. Acoustical configuration of Hot-wire microphone.

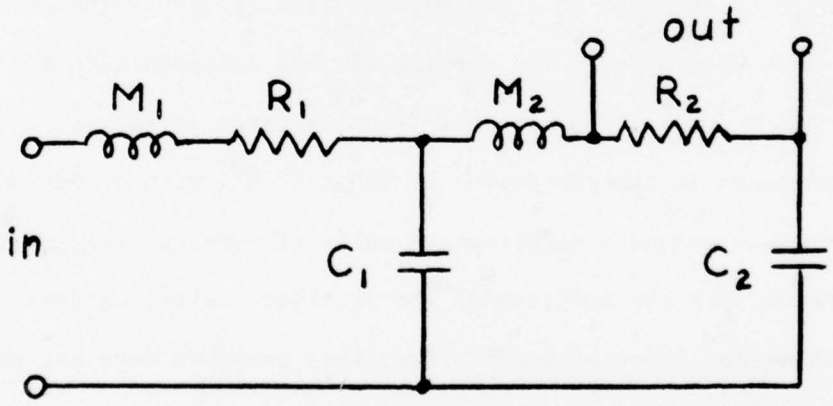

Figure 8. Equivalent electrical circuit for Hot-wire microphone. M and R are the acoustical inertance and resistance for the necks and C is the acoustical stiffness of the cavities.

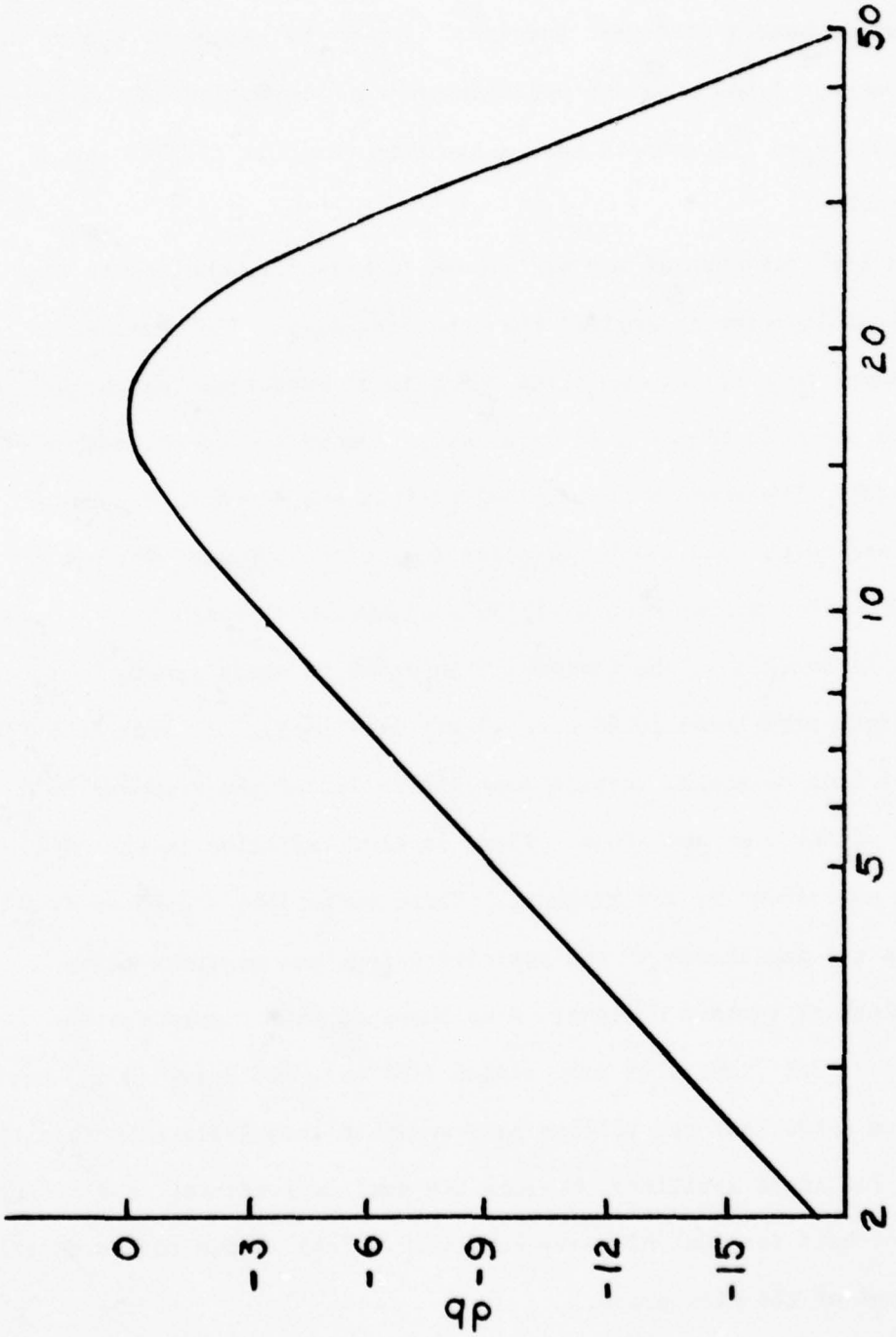

Figure 9. Frequency response of the T-23 microphone.

Some studies of low-frequency noise due to turbulence indicate that the spectrum falls off on the order of 6db/octave[5,6]. On the other hand, man-made noise due to battle would have a different spectrum. Since the explosive source as considered in Section I has a period approximately in proportion to the diameter of the bore, small arms fire should have a spectrum which is flat to about 900 Hz (.30 caliber).

The transient response of the microphone is more illuminating to the problem of determining time of arrival than the frequency. The response of the T-23 microphone to a triangular pulse which is an approximation to the explosive source shown in Figure 2 is obtained in Appendix C by the method of laplace transforms. The results for various periods are shown in Figure 10. The amplitudes are normalized so that a pulse length of 1000 msec (almost a Heaviside step for this microphone) will yield an output of unity.

As shown in Section I, the periods of interest in sound ranging vary from 10 msec (light artillery) to 30 msec (heavy artillery). As seen from Figure 10, these pulses have responses varying from 35% to 70% of the response to a 1000 msec pulse of the same amplitude. There is also variation in the amplitude of the negative over-shoot of the response. These variations are shown in Figure 11, where the amplitudes of the positive-going, and negative going responses to pulses of various periods. Also shown in this Figure are the approximate periods for light (105 mm), medium (155 mm), and heavy (8 in) artillery pulses. One notes that the valleys have somewhat less amplitudes than the peaks and that, for light artillery, besides the smaller pressures, the response is only about one-half for that of heavy artillery. This is due to the restricted frequency response of the microphone.

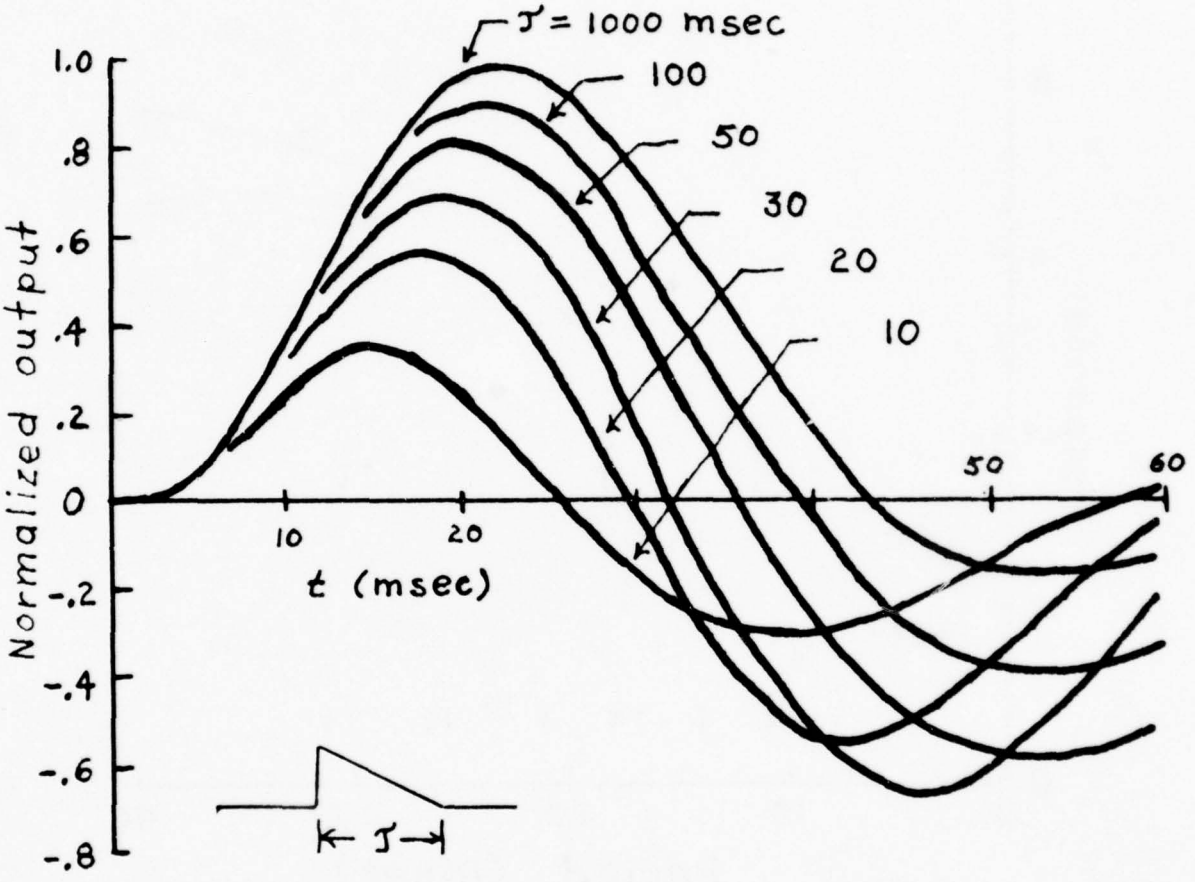

Figure 10: Response of T-23 microphone to a triangular pulse of width T.

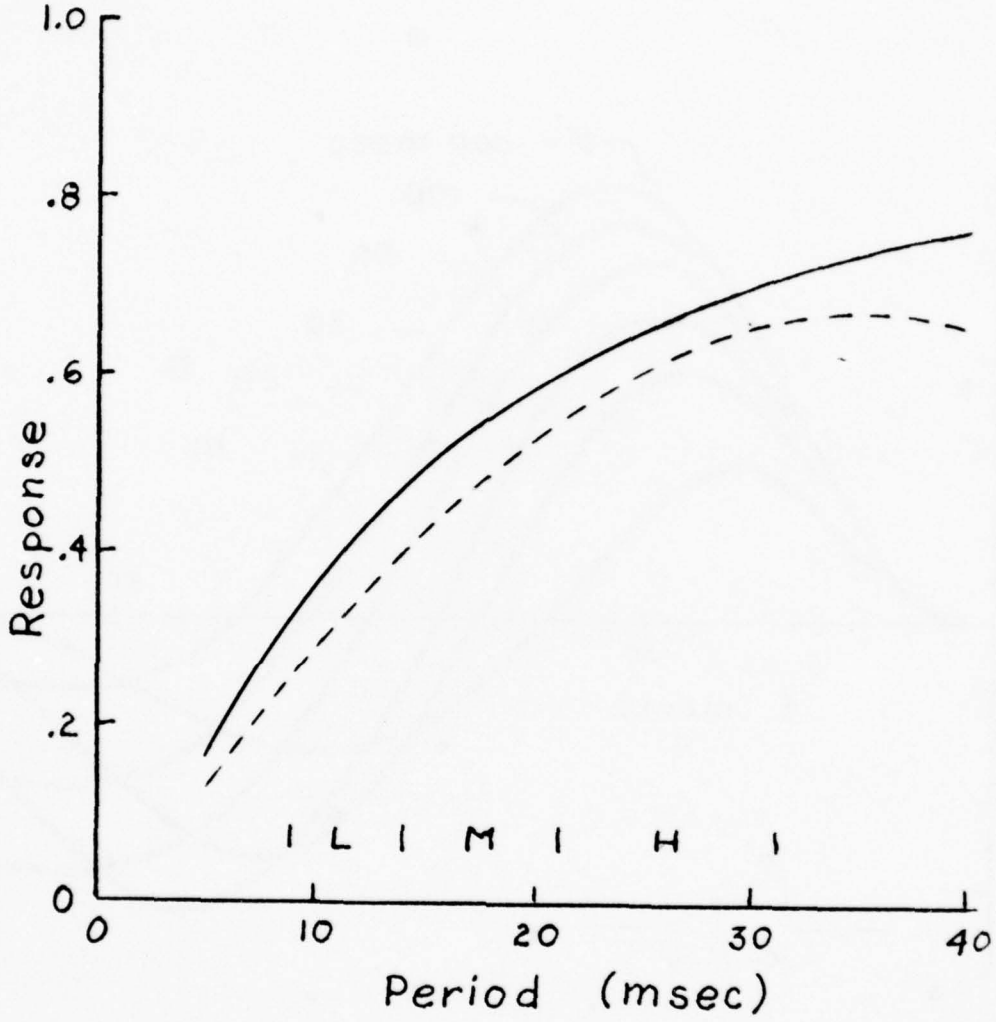

Figure 11. Response to unit triangular pulse of period T. The solid curve is the positive peak response, and the dashed curve is the negative peak response which follows. L, M, and H refer to light, medium, and heavy artillery.

Of course, one must see the signal in order to determine the location of the source, however, the time response to the pulse is critical in determining the arrival time. There are at present four points on the response curve which are used to determine the arrival time:

(1) The Break

(2) The Pressure Maximum

(3) The Cross-over

(4) The Pressure Minimum

The orthodox order of preference of these points is (1), (3), (2), and (4).[7]

One observes from Figure 10 that the break is difficult to determine in that, for all periods, there is very little signal for the first three msec. This is due to the sharp cut-off on the high-frequency side of the frequency response of the microphone. Assuming a noise of ± 0.05 ($S/N = 26db$) added to the response, the approximate deviations in determining the four points in time may be found to be:

Break = ±2 msec

Maximum = ±8 msec

Cross-over = ±3 msec

Minimum = ±10 msec

confirming the orthodox order, although the cross-over is almost equivalent to the break.

Unlike the detectable break, which lags about 3 msec behind the actual signal, the peak, cross-over, and valley lags depend on the period of the signal. This is seen in Figure 12, where the lag of these phases are shown as a function

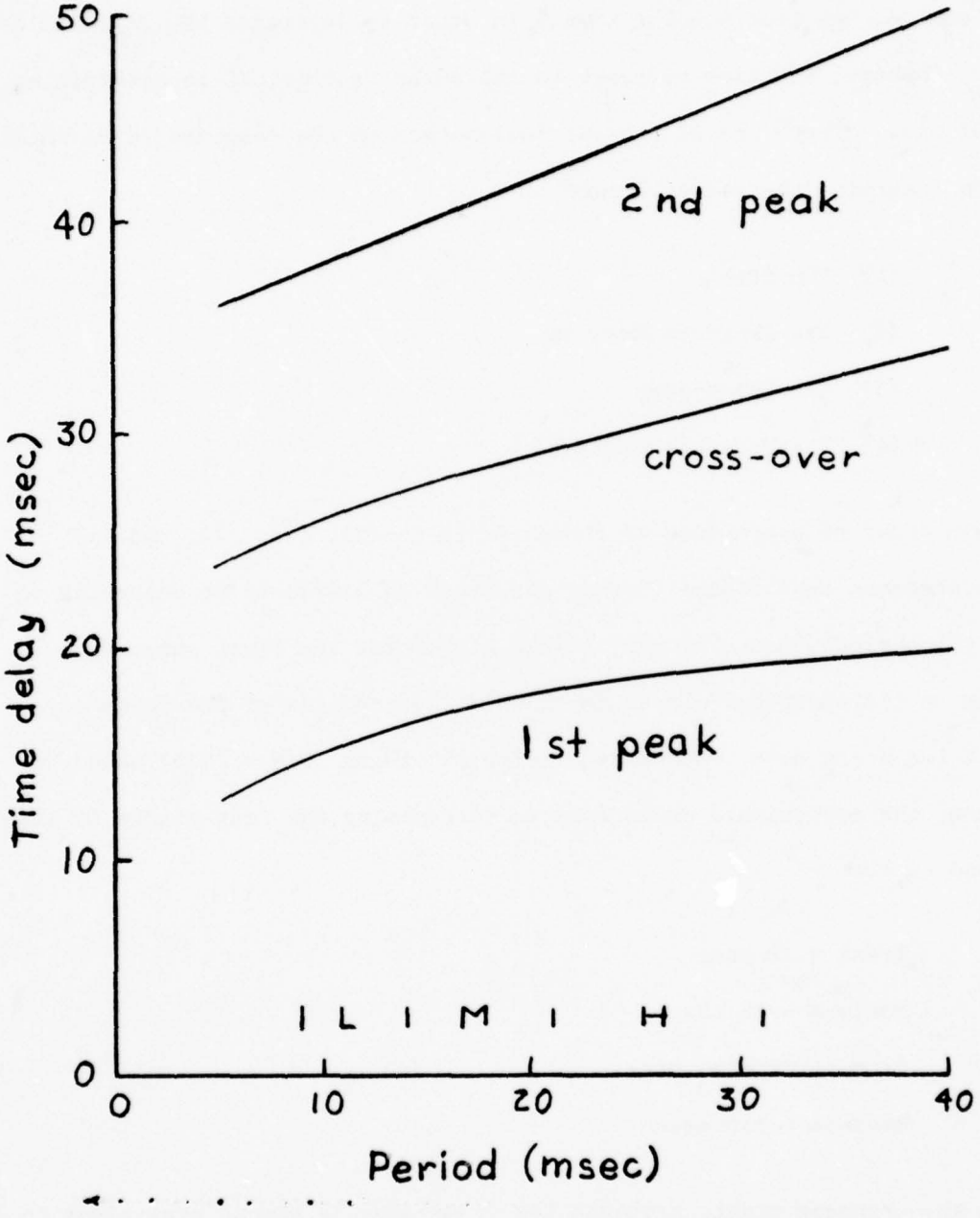

Figure 12. Time lags of the peak, crossover, and valley as functions of pulse period.

of the period of the pulse. It is seen, however, that the lags are fairly insensitive to the period; a change in period of 20 msec resulting in a change in lag of the valley (total length of signal) of only 10 msec. This insensitivity has two results: first, it makes it difficult to determine the period of the pulse and thus the type of artillery from the shape of the signal. Second, it allows the use of any of the three alternate phases (maximum, cross-over, and minimum) to be used as arrival times (assuming the same phase is used across the whole array). The maximum differential in pulse period across the array for a particular pulse would be for heavy artillery at short range (1 km). Table 2 shows this to be about 3 msec across the entire array for an extreme flanking angle. This results in only a variation of 1 1/2 msec for the valleys, with less for the peaks and cross-overs.

Thus, the use of a sharply peaked microphone has both advantages and drawbacks. Nearly all signals look about the same, which allows phase-comparison of signals, but the differences in input pulses are masked. In particular, the initial response to the signal is very slow, but the lag time is almost independent of the period of the input pulse. All this reminds one of Heisenberg's uncertainty principle -- and for good reason -- the product of the bandwidth of the microphone and the uncertainty of the arrival time of a pulse must be a constant for a particular signal-to-noise level.[8]

IV. RECOMMENDATIONS

Each of the foregoing sections are theoretical in nature and suggest experiments that would test the theory. The following recommendations stem directly from this investigation:

(1) A STUDY OF THE NATURE OF THE SOURCE SIGNAL. Although the triangular shaped waves due to explosions have been studied for sources that range from very large nuclear blasts to conventional TNT explosives, there may be questions still unanswered dealing with artillery. How symmetrical is the wave? Are there secondary shocks, creating "N" shaped waves? What is the exact relation between charge and bore to the period? These measurements require microphones with wide frequency responses, and these should be placed from about 500 m to several km from the sources. Also required would be meteorological data to confirm whether the propagation is diffracted or refracted. Some of the information sought in this study may already be available, but unknown to the author. The rise times associated with the received signals could answer the question of what is the effective specific acoustic impedance of certain types of terrain.

(2) A STUDY OF REFRACTIVE CORRECTIONS TO SOUND SPEED. The present method of weighting the vertical meteorological data appears ad hoc. Section II contains theory which indicates a method of weighting which could be programmed and the resulting locations be compared to the present method. Besides this test on already existant data, study (1) should yield actual travel times if timing is included. This

timing data could also indicate whether the surface meteorological or the presently used 200-m data is the more proper data to use in analysis.

(3) NOISE STUDIES. Arrival times could be improved by extending the response of the microphone and by increasing the dynamic range of the recorder. This is only true if the signal-to-noise ratio is not significantly decreased. There is very little known about the noise present underneath the wind screen. Here again, a wide-frequency response microphone is needed, along with wind speed data.

As mentioned in the introduction, an investigation of semi-automatic determination of arrival times has been made. This was done with an HP 9825 calculator with the input data digitized at a 5 msec sampling rate by hand. The calculator was able to detect the presence of signals by their magnitude to within about 10 msec. Closer analysis determined that although the breaks were difficult to detect, the peaks, cross-overs, and valleys were detected to within about a msec. In addition, cross-correlation of entire signals resulted in arrival time differences of less than one msec except for difficult signals.

A system compatible with such a calculator would acquire data with microphones with a flatter frequency response, and thus more information content. Since the algorithms used would not depend on hand calculations, the microphones could be placed in non-linear arrays, enabling distinction between forward and rear sources. The acquired data would be stored digitally on magnetic tape and displayed on CRT's. Operators would have the flexibility of filtering and amplifying the data for display.

The most efficient development of such a system would be by a team composed of people with expertise in the following areas:

(1) Field sound-ranging

(2) Microphones

(3) Computer hardware

(4) Computer software

(5) Atmospheric propagation of sound

(6) Information theory.

Some understanding of what the seismic industry has accomplished, and/or familiarity with the Navy's SONAR program would be helpful also.

Finally, it is quite possible that the biggest problem with sound ranging accuracy is the fact that meteorological data is obtained, by necessity, outside the area of interest and previous to the time of interest. However, this has yet to be proved, and therefore improvement in time-of-arrival determination is not necessarily an academic exercise.

ACKNOWLEDGMENT. The author appreciates the helpful comments of A. Blanco and S. L. Cohn. He is indebted to D. M. Swingle for his careful reading of and significant comments on this report.

REFERENCES

Literature Cited

1. W. E. Baker. Explosions in Air (University of Texas Press, Austin, 1973.)

2. H. L. Brode. Numerical solutions of spherical blast waves. Jour. Appl. Phys. 26, 766 (1955).

3. M. B. Wurlele and J. Roe. Problems and techniques of sound ranging. Final Report contract no. DAAD07-75-C-0087 (Dept. Atmospheric Sciences, U.C.L.A., 1977).

4. P. E. Doak. The reflexion of a spherical acauastical pulse by an absorbant plane. Proc. Royal Soc. 215A, 233-254 (1952).

5. E. A. Dean and G. G. Maxwell. The effect of turbulent pressure correlation of multiparts microphones. Contained in Third Quarterly Progress Report, Contract DA-36-039-AMC-03218(E) (Schellenger Research Laboratories, Univ. of Texas at El Paso, 1964).

6. G. G. Maxwell. An investigation of the nature and source of infrasonic noise in a wind field. Master's thesis. (Univ. of Texas at El Paso, 1966).

7. Artillery Sound Ranging and Flash Ranging. FM 6-122 (Department of the Army, Washington, D.C., 1964.)

8. See for instance C. W. Helstrom. Statistical theory of signal detection. (Pergamon Press, Oxford, England, 1968) ch. 5.

Selected Bibliography

1. E. A. Dean. A sound ranging system for the rocket grenade experiment at Wallops Island, Virginia. Final report NAS 5-221 (Schellenger Research Laboratory Univ. of Texas at El Paso, 1960).

2. T. G. Barnes. Ground support and data analysis and associated research and development for the rocket grenade experiment. Final report NAS 5-2949 (Schellenger Research Laboratories, Univ. of Texas at El Paso, 1965).

3. J. F. Casey. Ground support, data analysis and associated research and development for the rocket grenade experiement. Final report NAS 5-2949 (Schellenger Research Laboratories, Univ. of Texas at El Paso, 1965).

APPENDIX A

THE PROPAGATION OF A WEAK TRIANGULAR SHOCK

Suppose the waveform at some distance r_o from the source is similar to Fig. 2 and is given by

$$P(x) = \begin{cases} 0 & , \quad x < 0 \\ P_o(1 - x/L_o) & , \quad 0 < x < L_o \\ 0 & , \quad x < L_o . \end{cases} \tag{A1}$$

As the shock propagates, the pulse length increases since the shock at x=0 travels faster than the point at $x = L_o$. The rate of change of L is given by

$$\frac{dL}{dr} = \frac{dL}{dt}\frac{dt}{dr} \approx \frac{1}{c}\frac{dL}{dt} , \tag{A2}$$

where c is the sound speed. The velocity of the shock is given by

$$v^2 = c^2(1 + \frac{\gamma+1}{2\gamma}\frac{P}{p_o}), \tag{A3}$$

where γ is the ratio of specific heats, P is the differential shock pressure and p_o is the ambient pressure. For weak shocks $P/p_o \ll 1$ and

$$v \approx c(1 + \frac{\gamma+1}{4\gamma}\frac{P}{p_o}) \tag{A4}$$

thus

$$\frac{dL}{dt} = c(1 + \frac{\gamma+1}{4\gamma}\frac{P}{p_o}) - c, \tag{A5}$$

since the end of the pulse, having no overpressure, travels at the speed c. Eq. (A5) substituted into Eq. (A2) yields

$$\frac{dL}{dr} = \frac{\gamma+1}{4\gamma}\frac{P}{p_o} . \tag{A6}$$

The total energy of the shock wave may be obtained by integrating the

energy density

$$u = \frac{P^2}{\rho c^2} , \tag{A7}$$

where ρ is the density of the medium, over the entire volume of the wave. Assuming spherical propagation, this becomes

$$E = \frac{4\pi r^2 p^2}{\rho c^2} \int_o^x (1 - \frac{x}{L})^2 dx, \tag{A8}$$

$$= \frac{4\pi r^2 p^2 L}{3\rho c^2} . \tag{A9}$$

If energy were conserved, one could solve Eq. (A9) for P(r,L), substitute into Eq. (A6) and integrate. There is, however, an increase in entropy across the shock which depends on the third power of the pressure difference across the shock[1]

$$\Delta S = \frac{1}{T} \left(\frac{\partial^2 V}{\partial p^2} \right)_S \frac{P^3}{12} , \tag{A10}$$

where S is entropy, T is absolute temperature, and V is volume. For an ideal gas,

$$\left(\frac{\partial 2_V}{\partial p^2} \right)_S = \frac{\gamma+1}{\gamma^2} \frac{V}{p^2} , \tag{A11}$$

where the adiabatic relation pV^γ = coust has been used. Substitution of Eq. (A11) into (A10) results in

$$\Delta S = \frac{nR(\gamma+1)}{12\gamma^2} \left(\frac{P}{p_o} \right)^3 , \tag{A12}$$

where the equation of state pV = nRT has been called upon. The number of moles is n and R is the gas constant.

The rate change of entropy with distance is

$$\frac{dS}{dr} = \frac{dS}{dt}\frac{dt}{dr} = \frac{1}{c}\frac{dS}{dt}$$

$$= \frac{R(\gamma+1)}{12\gamma^2 C}\left(\frac{P}{p_o}\right)^3 \frac{dn}{dt} , \qquad \text{(A13)}$$

where dn/dt is the rate of flow (in moles) across the shock. Again assuming spherical propagation,

$$\frac{dn}{dt} = 4\pi r^2 \frac{c\rho}{M} , \qquad \text{(A14)}$$

where $c\rho$ is the max flux and M is the molecular mass. Thus

$$\frac{dS}{dr} = \frac{4\pi r^2(\gamma+1)P^3}{12\gamma^2 p_o^{\ 2} T} , \qquad \text{(A15)}$$

where the ideal gas relation $\rho = pM/RT$ has been used.

The rate of energy loss is $dE = -TdS$, or

$$\frac{dE}{dr} = -\frac{4\pi r^2(\gamma+1)\ P^3}{12\gamma^2 p_o^{\ 2}} , \qquad \text{(A16)}$$

Division by Eq. (A9) leads to

$$\frac{1}{E}\frac{dE}{dr} = -\frac{(\gamma+1)\rho c^2\ P}{4\gamma^2 p_o^{\ 2} L} \qquad \text{(A17)}$$

or

$$\frac{1}{E}\frac{dE}{dr} = -\frac{\gamma+1}{4}\left(\frac{P}{p_o}\right)\frac{1}{L} , \qquad \text{(A18)}$$

where $c^2 = \gamma\ p_o/\rho$ has been used to simplify. Thus

$$\frac{1}{E}\frac{dE}{dr} = -\frac{1}{L}\frac{dL}{dr} , \qquad \text{(A19)}$$

which, upon integration yields the remarkably simple result

$$EL = \text{constant}. \tag{A20}$$

Thus

$$\frac{4\pi r_o^2 P_o^2 L_o^2}{3\rho c^2} \approx \frac{4\pi r^2 P^2 L^2}{3\rho c^2}, \tag{A21}$$

or

$$P = P_o \frac{r_o}{r} \frac{L_o}{L}, \tag{A22}$$

which, when substituted int Eq. (A6) becomes

$$\frac{1}{L_o}\int_{L_o}^{L} L dL = \frac{\gamma+1}{4\gamma} \frac{P_o r_o}{p_o} \int_{r_o}^{r} \frac{dr}{r}, \tag{A23}$$

or

$$L = \{L_o[L_o + \frac{\gamma+1}{2\gamma} \frac{P_o}{p_o} r_o \ell n(r/r_o)]\}^{\frac{1}{2}}. \tag{A24}$$

The above derivation has considered the increase in entropy due to the finite amplitude of the shock, but has neglected the increase in entropy due to viscothermal and molecular relaxation effects. The absorption of sound in air is frequency dependent and highly sensitive to humidity. High frequencies are attenuated more rapidly than low, resulting in a rounding off of the initial pressure peak.

REFERENCES

1. L. D. Landau and E. M. Lifshitz. Fluid Mechanics (Pergaman Press, Oxford, England 1959), p. 323.

APPENDIX B

MEAN SOUND SPEED FOR WAVES REFRACTED BY CONSTANT GRADIENTS IN SOUND SPEED AND WIND VECTOR

If θ is the elevation angle of a sound ray (normal to a wave front) and ϕ is the azimuth angle, then the law of refraction yields[1]

$$\left.\begin{aligned} \phi &= \phi_o, \\ \frac{c_p}{\cos\theta} &= \frac{c_{p_o}}{\cos\theta_o} \end{aligned}\right\} \tag{B1}$$

where θ_o and ϕ_o are the original source values for the ray and c_p is the phase velocity of sound. The first equation demands that the azimuth angle is constan and the second is Snell's law of refraction. In a moving medium, the phase velocity is

$$c_p = c + \hat{n}\cdot\vec{w} , \tag{B2}$$

where c is the sound speed in a nonmoving medium, n is the unit vector in the direction of the ray, and w is the wind velocity vector (the velocity of the moving medium). This is in contrast to the group velocity

$$\vec{c}_g = c\hat{n} + \vec{w} , \tag{B3}$$

which is the velocity of energy propagation.

Since, for a particular ray, ϕ is fixed, the wind vector may be resolved into two components: u in the direction of and v normal to $\hat{n}$. Thus Eq. (B1) becomes

$$\frac{c + u\cos\theta}{\cos\theta} = \frac{c_o + u_o\cos\theta_o}{\cos\theta_o} \tag{B4}$$

If the atmosphere is considered to have linear gradients for c and w,

$$c = c_o(1 + az),$$

$$u = u_o + c_o bz \tag{B5}$$

$$v = v_o + c_o dz$$

where a, b, and d are constants with units of $(\text{length})^{-1}$. Thus Eq. (B4) has the solution

$$\cos\theta = \cos\theta_o \frac{1 + az}{1 - bz\cos\theta_o} . \tag{B6}$$

If the additional assumption $bz\cos\theta_o << 1$ is made, then Eq. (B) becomes, to the first order

$$\cos\theta = \cos\theta_o[1 + (a + b\cos\theta_o)z]. \tag{B7}$$

The above assumption requires that the total change in wind speed over the path of the ray is much less than the sound speed itself. Eq. (B7) may be solved for z

$$z = \frac{\cos\theta - \cos\theta_o}{(a + b\cos\theta_o)\cos\theta_o} , \tag{B8}$$

and thus

$$dz = -\frac{\sin\theta\, d\theta}{(a + b\cos\theta_o)\cos\theta_o} . \tag{B9}$$

The velocity of the ray's tip is given by the group velocity

$$\frac{dx}{dt} = c\cos\theta + u,$$

$$\frac{dy}{dt} = v, \tag{B10}$$

$$\frac{dz}{dt} = c\sin\theta ,$$

$$\frac{dx}{dt} = c\cos\theta + u,$$

$$\frac{dy}{dt} = v, \tag{B10}$$

$$\frac{dz}{dt} = c\sin\theta,$$

where x is in the ϕ-direction, y is normal to the ϕ-direction, and z is up. It is clear that the ray reaches its maximum height Z when $\theta = 0$, and that the path is symmetric with respect to this position. Thus, since

$$\frac{dx}{dz} = \frac{\cos\theta}{\sin\theta} + \frac{u}{c\sin\theta}, \tag{B11}$$

then

$$X = 2\int_o^z \frac{\cos\theta}{\sin\theta} + \frac{u}{c\sin\theta}\, dz, \tag{B12}$$

where X is the x-coordinate of the point of arrival of the ray back at the surface. (See Fig. B1). Eq. (B9) simplifies this to

$$X = \frac{2}{(a + b\cos\theta_o)\cos\theta_o}\left[\int_o^{\theta_o} \cos\theta d\theta + \int_o^{\theta_o} \frac{u}{c}\, d\theta\right]. \tag{B13}$$

The first integral in Eq. (B13) is simple and the second is much smaller (since $u/c<<1$), allowing for the approximation

$$\frac{u}{c} = \frac{u_o + c_o bz}{c_o(1 + az)} \approx \frac{u_o}{c_o} + bz. \tag{B14}$$

Eq. (B14) combined with (B13) yields

$$X = \frac{2}{(a + b\cos\theta_o)\cos\theta_o}\left[\sin\theta_o + \frac{u_o\theta_o}{c_o} + \frac{b}{a + b\cos\theta_o}(\tan\theta_o - \theta_o)\right]. \tag{B15}$$

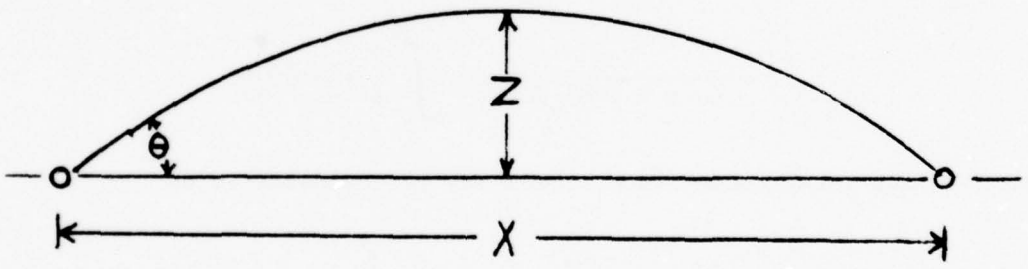

Figure B1. Geometry of refracted ray.

Assuming that $\theta_o << 1$, this simplifies to

$$X = \frac{2\theta_o}{a+b}\left[1 + \frac{2a + 7b}{6(a + b)}\,\theta_o^2 + \frac{u_o}{c_o}\right] , \tag{B16}$$

where terms beyond θ^3 have been neglected in the trigonometric expansions.

Following the same arguments,

$$Y = \frac{2\theta_o}{a+b}\left[\frac{d}{6(a + b)}\,\theta_o^2 + \frac{v_o}{c_o}\right] , \tag{B17}$$

where Y is the net displacement of the ray in the y-direction.

Thus the x and y components of the ray have been found. The mean speed is this displacement divided by the travel time. The time of travel is obtained from integrating

$$dt = \frac{dz}{c\,\sin\theta} , \tag{B18}$$

or, with the use of Eq. (B9),

$$T = \frac{2}{(a + b\,\cos\theta_o)\cos\theta_o}\int_o^{\theta_o} \frac{d\theta}{c(1 + az)} , \tag{B19}$$

where T is the total travel time. This may be approximated by

$$T = \frac{2}{c_o(a + b\,\cos\theta_o)\cos\theta_o}\int_o^{\theta} (1 - az)\,d\theta, \tag{B20}$$

which becomes, with the use of Eq. (B8)

$$T = \frac{2\theta_o}{c_o(a + b\,\cos\theta_o)\cos\theta_o}\left[1 - \frac{a(\tan\theta_o - \theta_o)}{a + b\,\cos\theta_o}\right] , \tag{B21}$$

or, for small θ_o,

$$T = \frac{2\theta_o}{c_o(a + b)}\left[1 + \frac{a + 6b}{6(a + b)}\,\theta_o^2\right] . \tag{B22}$$

The mean speed in the x-direction is thus

$$\langle v_x \rangle = \frac{X}{T} = c_o \left[1 + \frac{\theta_o^2}{6} + \frac{u_o}{c_o} \right] , \tag{B23}$$

and the mean speed in the y-direction is

$$\langle v_y \rangle = \frac{Y}{T} = c_o \left[\frac{v_o}{c_o} + \frac{d\theta_o^2}{6} \right] . \tag{B24}$$

These equations are the mean speeds for a ray leaving the surface at an elevation θ_o and arriving at (X,Y) at time T. The results depend on a linear gradient in c and w which is not too steep and they are correct to the second power of θ_o.

One must now replace θ_o with the proper function of the distance between source and receiver, since θ_o is not generally known. The total distance travelled by the ray (measured along the surface) is

$$R = (X^2 + Y^2)^{\frac{1}{2}} = \frac{2\theta_o}{a + b} \left[1 + \frac{2a + 7b}{6(a + b)} \theta_o^2 + \frac{u_o}{c_o} \right]^{\frac{1}{2}} , \tag{B25}$$

correct to order θ_o^3 and to first power in u_o/c_o. Thus

$$\theta_o = \tfrac{1}{2}(a + b)R, \tag{B26}$$

correct to order R^2. This yields

$$\langle v_x \rangle = c_o [1 + \frac{u_o}{c_o} + \frac{1}{24} (a + b)^2 R^2] , \tag{B27}$$

and

$$\langle v_y \rangle = c_o \left[\frac{v_o}{c_o} + \frac{d}{24} (a + b)R^2 \right] . \tag{B28}$$

The maximum height obtained by the ray is given by

$$Z = \frac{1 - \cos\theta_o}{(a + b \cos\theta_o)\cos\theta_o} , \tag{B29}$$

or, for small θ_o,

$$Z = \frac{\theta_o^2}{2(a + b)} \tag{B30}$$

Thus retaining terms of order $\theta_o^2/(a+b)$, which has been done, corresponds to retaining terms linear in z, consistant with the constant-gradient atmospheric model. Finally, it may be noted that Eq. (B30) may be written

$$Z = \frac{1}{8} (a + b)R^2, \tag{B31}$$

giving the maximum height in terms of the range and the gradients.

The substitution of Eq. (B31) into (B27) yields

$$\langle v_x \rangle = c_o[1 + \frac{u_o}{c_o} + \frac{1}{3} (a + b)Z],$$

$$= c(\frac{Z}{3}) + u(\frac{Z}{3}), \tag{B32}$$

or, the mean speed in the x-direction is the speed evaluated at Z/3, one-third of the maximum height. Likewise Eq. (B28) becomes

$$\langle v_y \rangle = c_o[\frac{v_o}{c_o} + \frac{1}{3} dZ]$$

$$= v(\frac{Z}{3}) \tag{B33}$$

or, the cross-wind evaluated at 1/3 of the maximum height.

REFERENCES

1. R. B. Lindsay. Mechanical Radiation (McGraw-Hill, New York, 1960) p. 298.

APPENDIX C. T-23 MICROPHONE FREQUENCY AND PULSE RESPONSE

The T-23 double resonator hot wire microphone has the acoustical configuration shown in Figure 7. The analogous electrical circuit is shown in Figure 8. This circuit is composed of elements defined to be:

M = Inertance of neck,

R = Acoustical resistance of neck

C = Compliance of cavity,

$= V/\rho c^2 = V/\gamma p$

where γ is the ratio of specific heats and p is the ambient pressure. The subscripts refer to the upper resonator (1) and the lower resonator (2). The acoustic pressure incident on the microphone is P(t) and the volume velocity flowing through the necks is U(t).

For $P(t) = P_o e^{i\omega t}$, the loop equations are:

$$P_o = i\omega M_1 U_1 + R_1 U_1 - i \frac{U_1 - U_2}{\omega C_1}$$

$$0 = i\omega M_2 U_2 + R_2 U_2 - i \frac{U_2}{\omega C_2} - i \frac{U_2 - U_1}{\omega C_1} \qquad \text{(C1)}$$

where U_1 and U_2 are the amplitudes of the volume velocities through the necks.

Since the output is proportional to U_2, the relative response of the microphone is given by

$$\frac{U_2}{P_o} = \frac{1}{Z} , \qquad \text{(C2)}$$

where Z is the effective acoustical impedance. The solution to the set of equations (C1) yields

$$Z = R' + i\omega M' - i\,\frac{1}{\omega C_2} \tag{C3}$$

where

$$R' = R_1\left(1 + \frac{C_1}{C_2} - \omega^2 M_2 C_1\right) + R_2\left(1 - \omega^2 M_1 C_1\right), \tag{C4}$$

and

$$M' = M_1\left(1 + \frac{C_1}{C_2} - {}^{2}M_2^2 C_1\right) + M_2 + R_1 R_2 C_1. \tag{C5}$$

The output voltage is thus,

$$E_o = 20\,\log(K/|Z|)\ \text{db}, \tag{C6}$$

where K is a constant of proportionality and $|Z|$ is the absolute value of the complex impedance. The phase angle of the output with respect to the input is,

$$\theta = \tan^{-1}(-X'/R'), \tag{C7}$$

where,

$$X' = \omega M' - \frac{1}{\omega C_2} \tag{C8}$$

The acoustical impedance of a small tube is[1]

$$Z_t = \frac{L}{\pi r^2}\left(\frac{8\mu}{r^2} + \frac{4}{3}\,i\omega\rho\right), \tag{C9}$$

where L and r are the length and radius of the tube, μ is the viscosity of the air, and ρ is the density of the air. The criteria for smallness depends on the thickness of the viscous boundary layer which, in turn, depends on the frequency of the signal. In addition, the effect of the impedance miss-match between the infinite medium and the tube is sometimes approximated by adding a correction to the length of

$$\Delta L = \frac{16r}{3\pi}\ . \tag{C10}$$

The volumes of the cavities and the characteristics of the necks have been measured.[2] Using $C = V/\gamma p$ and Eqs. (C9) and (C10),

$$C_1 = 1.9 \times 10^{-3} \text{ cm}^5/\text{dyne}$$

$$C_2 = 0.7 \times 10^{-3} \text{ cm}^5/\text{dyne}$$

$$R_1 = 3.4 \text{ acoustical ohms},$$

$$R_2 = 30 \text{ acoustical ohms},$$

$$M_1 = 3.8 \times 10^{-2} \text{ gm/cm}^4$$

$$M_2 = 8.2 \times 10^{-2} \text{ gm/cm}^4$$

In the above, the characteristics of the 25 Hz plug in the top neck has been assumed. *Since the tubes in this case are somewhat thicker than the boundary* layer, the values for R and M should be reduced.

Figure C1 shows the relative response of several T-23 microphones.[3] This response was measured in a pistonphone and is accurate to within about ±1 db. The solid line beyond about 17 Hz is calculated from the above values, and is seen to be an accurate representation of the measured response. For less than about 17 Hz, there are two lines shown. The dashed line is the calculated response using the values determined above. The solid line is an empherical fit to the data using:

$$R_1 = 2.4 \text{ acoustical ohms},$$

$$R_2 = 20 \text{ acoustical ohms},$$

$$M_1 = 3.6 \times 10^{-2} \text{ gm/cm}^4$$

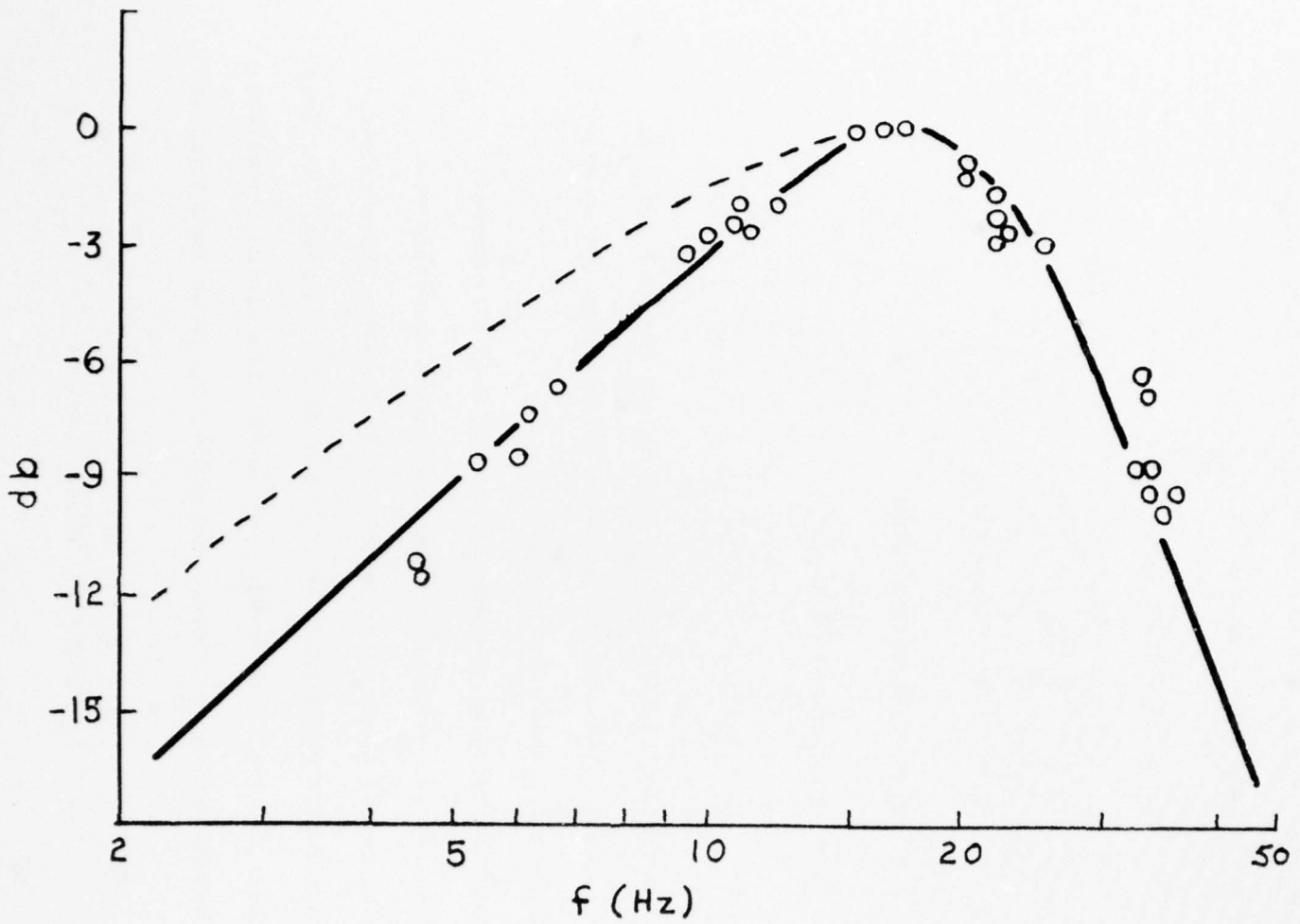

Figure C1. The frequency response of the T-23 microphone. Circles indicate measured values for four different microphones. The solid curve indicates the theoretical response with the impedance of the neck's empirically adjusted to fit the measured data. The dashed curve indicates theory without adjustment for the finite diameter of the necks.

$$M_2 = 7.8 \times 10^{-2} \text{ gm/cm}^4,$$

assuming that R and M should be decreased due to the finite radius of the tubes.

As may be seen from Figure C1, the above empirical values closely fit the observed response curve. However, in the case of sounding ranging, the important response is characterized by the response to a triangular-shaped explosive pulse, rather than a sine wave. The response to a pulse is obtained from a Laplace transform of the circuit. This is obtained from the frequency response by substituting s for $i\omega$:

$$\frac{L[P(t)]}{L[E(t)]} = s^3(M_1M_2C_1) + s^2(M_1R_2C_1 + M_2R_1C_1) + s(M_1 + M_1C_1/C_2 + R_1R_2C_1 + M_2)$$

$$+ R_1 + R_1C_1/C_2 + \frac{1}{s}\left(\frac{1}{C_2}\right), \qquad \text{(C11)}$$

where $L[\ ]$ indicates the Laplace transform. Some algebraic manipulations yield

$$L[E(t)] = L[P(t)] \cdot \frac{C_2\omega_1^2\omega_2^2 s}{f(s)}, \qquad \text{(C12)}$$

where $\omega_1^2 = \frac{1}{M_1C_1}$, $\omega_2^2 = \frac{1}{M_2C_2}$, and

$$f(\ ) = s^4 + (\delta_1 + \delta_2)s^3 + (\omega_1^2 + \omega_2^2 + \omega_{12}^2 + \delta_1\delta_2)s^2$$

$$+ (\delta_1\omega_{12}^2 + \delta_1\omega_2^2 + \delta_2\ 1^2)s + \omega_1^2\omega_2^2, \qquad \text{(C13)}$$

and

$$\omega_{12}^2 = 1/M_2C_1,\ \delta_1 = R_1/M_1 \text{ and } \delta_2 = R_2M_2.$$

If one defines $x = s/\omega_{12}$, then Eq. (C13) becomes

$$g(x) = \omega_{12}^4[x^4 + a_3x^3 + a_2x^2 + a_1x + a_o], \qquad \text{(C14)}$$

where

$$\left.\begin{aligned} a_3 &= \frac{\gamma_1 + \gamma_2}{\gamma_{12}}, \\ a_2 &= \frac{\gamma_1^2 + \gamma_2^2 + \gamma_{12}^2 + \gamma_1\gamma_2}{\gamma_{12}^2} \\ a_1 &= \frac{\delta_1\omega_{12}^2 + \delta_1\omega_2^2 + \delta_2\omega_1^2}{\omega_{12}^3} \\ a_o &= \frac{\omega_1^2\omega_2^2}{\omega_{12}^2} \end{aligned}\right\} \qquad \text{(C15)}$$

We wish to factor the quartic Eq. (C14) by Ferrari's method. The first step is to obtain the resolvent cubic

$$y^3 - a_2y^2 + (a_1a_3 - 4a_o)y - (a_1^2 + a_oa_3^2 - 4a_oa_2). \qquad \text{(C16)}$$

For the case at hand,

$$a_3 \approx 4.09,$$

$$a_2 \approx 8.54,$$

$$a_1 \approx 10.12,$$

$$a_o \approx 5.88,$$

which, by numerical methods yields a real solution y = 4.857. This solution results in resolving the quartic into two quadratic equations[4]

$$\frac{g(k)}{\omega_{12}^4} = (x^2 + c_1^{(+)}x + c_2^{(+)})(x^2 + c_1^{(-)}x + c_2^{(-)}), \qquad \text{(C17)}$$

where

$$c_1^{(\pm)} = \frac{a_3}{2} \pm \left(\frac{a_3^2}{4} + y - a_2\right)^{1/2},$$

$$c_2^{(\pm)} = \frac{y}{2} \pm \left(\frac{y^2}{4} - a_o\right)^{1/2},$$

or

$$c_1 = 2.75,\ 1.34,$$

$$c_2 = 2.30,\ 2.56.$$

More algebraic manipulations result in

$$e(s) = \frac{sp(s)}{\phi_1(s)\phi_2(s)} \quad , \tag{C18}$$

for Eq. (C12) where $e(s) = L[E(t)]$, $p(s) = L[P(t)]$, and

$$\phi_1 = (x + a_1)^2 + b_1^2,$$

$$\phi_2 = (s + a_2)^2 + b_2^2,$$

and where

$$a_1 = 112.9,$$
$$a_2 = 55.0,$$
$$b_1 = 52.5,$$
$$b_2 = 120.1.$$

Assuming a triangular pulse for P(t),

$$P(t) = \begin{cases} 0 & , t < 0 \\ 1 - t/T & , 0 \geq t \geq T \\ 0 & , t > T \ , \end{cases} \tag{C19}$$

then

$$L[P(t)] = p(s) = \int_o^T (1 - t/T)e^{-st}dt, \tag{C20}$$

or, upon integration,

$$p(s) = \frac{1}{s}\left(1 - \frac{1}{TS} + \frac{1}{TS}e^{-sT}\right). \tag{C21}$$

Substitution into Eq. (C18) yields

$$e(s) = e_1(s) + e_2(s) + e_3(s), \tag{C22}$$

where

$$e_1(s) = \frac{1}{\phi_1(s)\phi_2(s)} ,$$

$$e_2(s) = -\frac{1}{Ts\phi_1(s)\phi_2(s)} ,$$

$$e_3(s) = \frac{e^{-sT}}{Ts\phi_1(s)\phi_2(s)} .$$

Considering $e_1(s)$ first, this may be written

$$e_1(s) = \frac{A_1 + B_1 s}{\phi_1(s)} + \frac{A_2 + B_2 s}{\phi_2(s)} \tag{C23}$$

A table of Laplace transforms then yields

$$E_1(t) = \frac{e^{-a_1 t}}{b_1 c_1^2}\left[p_{r1}\sin b_1 t - p_{i1}\cos b_1 t\right] + \frac{e^{-a_2 t}}{b_2 c_2^2}\left[p_{r2}\sin b_2 t - p_{i2}\cos b_2 t\right], \tag{C24}$$

where

$$p_{r1} = (a_2 - a_1)^2 + b_2^2 - b_1^2,$$

$$p_{i1} = 2b_1(a_2 - a_1),$$

$$c_1^2 = (a_2 - a_1)^2 + b_2^2 + b_1^2 - 4b_1^2 b_2^2,$$

$$p_{r2} = (a_1 - a_2)^2 + b_2^2 + b_1^2 - 4b_1^2 b_2^2,$$

$$p_{i2} = 2b_2(a_1 - a_2),$$

$$c_2^2 = c_1^2.$$

This portion of the response of the microphone is that due to a unit step function, and is shown, normalized to unity, in Fig. C2.

Next, considering $e_2(s)$,

$$e_2(s) = -\frac{1}{Ts} e_1(s), \tag{C25}$$

which becomes

$$E_2(t) = -\frac{1}{T} \int_o^t E_1(y)dy, \tag{C26}$$

upon taking the transform. Integration yields

$$E_2(t) = -\frac{1}{a_1^2 + b_1^2}\left\{e^{-a_1 t}\left[(Bb_1 - Aa_1)\sin b_1 t - (Ba_1 + Ab_1)\cos b_1 t\right] + \frac{Ab_1 + Ba_1}{a_1^2 + b_1^2}\right.$$

(Eq. cont. on next page)

$$- \frac{e^{-a_2 t}}{a_2^2 + b_2^2} [(Bb_2 - Ca_2)\sin b_2 t$$

$$- (Ba_2 + Cb_1)\cos b_2 t] + \frac{Cb_2 + Ba_2}{a_2^2 + b_2^2} \Bigg\} , \qquad \text{(C27)}$$

where, for this case,

$$A = 6.19$$

$$B = 2.51$$

$$C = 1.50.$$

This function, the response to the triangular portion of the pulse, is shown in Fig. C3, with the same normalization as $E_1(t)$.

Finally, the last term may be resolved by the use of

$$F(t - T) = L^{-1} e^{-Ts} f(s), \qquad \text{(C28)}$$

yielding

$$E_3(t) = \begin{cases} 0 & , \quad t \leq T \\ -E_2(t - T) & , \quad t > T \end{cases} . \qquad \text{(C29)}$$

The required function $E_1(t)$ and $E_2(t)$ are tabulated in Table C1.

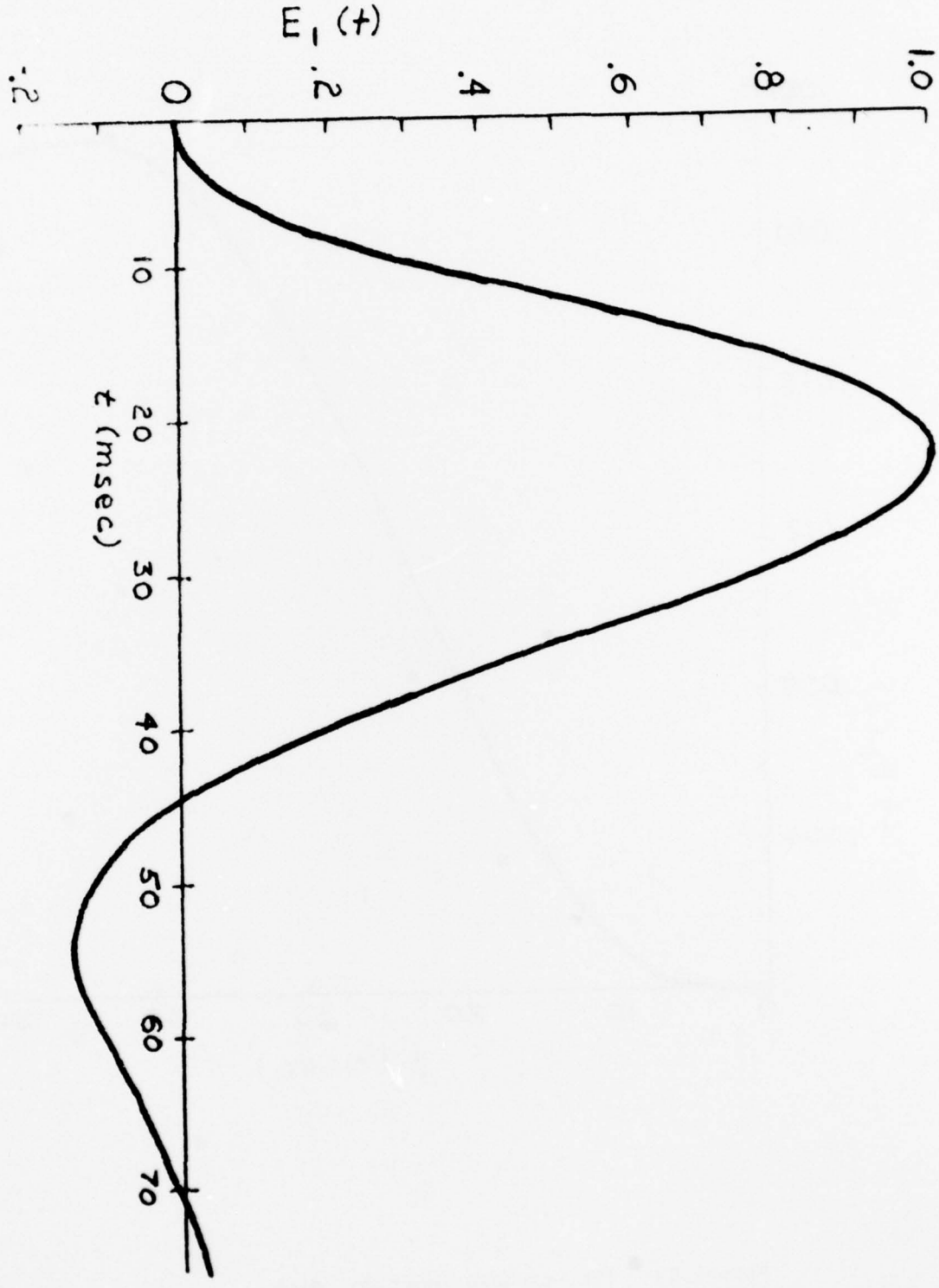

Figure C2. The response function E(t).

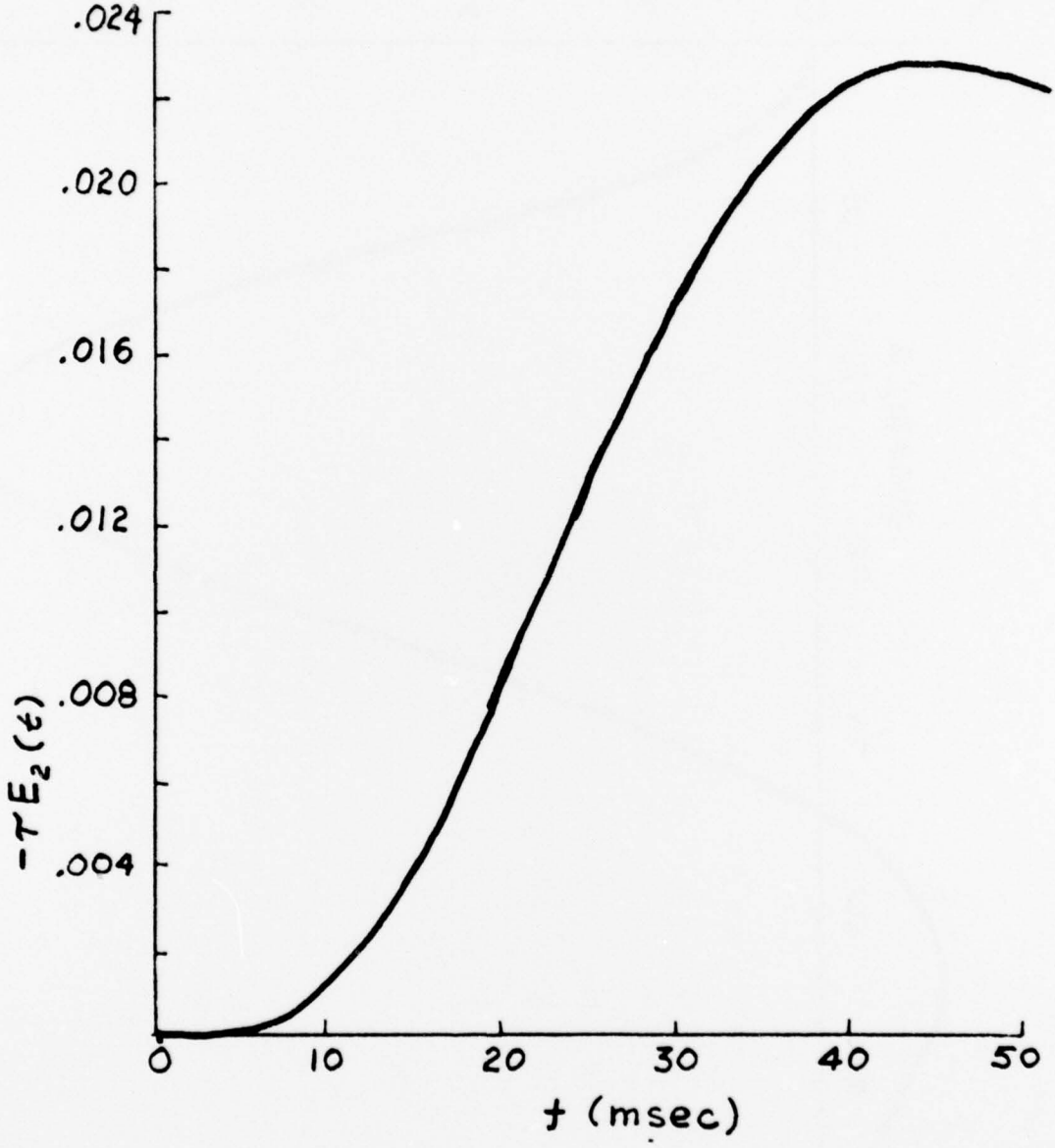

Figure C3. The response function $E_2(t)$

Table C1. Response functions for the T-23 microphone. Functions are normalized so that $E_1(T)_{max} = 1.000$. The response to a triangular pulse of duration T is $E(t) = E_1(t) + E_2(t) + E_3(t)$, where $E_3(t) = 0$ for $t \leq T$, and $E_3(t) = -E_2(t - T)$ for $t > T$.

tim (msec)	$E_1(t)$ (volts)	$TE_2(t)$ (volt·sec)
0	.000	.0000
5	.076	-.0001
10	.376	-.0012
15	.74	-.0040
20	.97	-.0084
25	.97	-.0133
30	.77	-.0177
35	.47	-.0208
40	.18	-.0224
45	-.02	-.0228
50	-.12	-.0224
55	-.14	-.0217
60	-.10	-.0211
65	-.05	-.0207
70	.00	-.0206
75	.03	-.0207
80	.03	-.0208
85	.03	-.0210
90	.01	-.0211

REFERENCES

1. H. F. Olson, Elements of Acoustical Engineering, 2nd Edition (D. Van Nootrand, Princeton, 1947).

2. E. A. Dean and J. G. Pruitt, Sound Ranging for the Rocket Grenade Experiment, Quarterly progress report no. 2, NAS 5-556. (Schellenger Research Laboratories, University of Texas at El Paso, 1962).

3. E. A. Dean, J. G. Pruitt, and L. L. Chapin. Sound Ranging for the Rocket-Grenade Experiment. Quarterly progress report no. 1, NAS 5-556. (Schellenger Research Laboratories, University of Texas at El Paso, 1961).

4. M. Abramouritz and I. A. Stegun. Handbook of Mathematical Functions. (Dover, New York, 1965) Section 3.8.3. Note that there is a misprint. One of the signs should be 1.

☆ U.S. GOVERNMENT PRINTING OFFICE: 1979 — 677-017/7